(12) INTERNATIONAL APPLICATION PUBLISHED UNDER THE PATENT COOPERATION TREATY (PCT)

(19) World Intellectual Property Organization
International Bureau

(43) International Publication Date
6 November 2014 (06.11.2014)

WIPO | PCT

(10) International Publication Number
WO 2014/176663 A1

(51) International Patent Classification:
G01R 33/31 (2006.01) *G01R 33/30* (2006.01)
A61B 5/055 (2006.01)

(21) International Application Number:
PCT/CA2014/000066

(22) International Filing Date:
31 January 2014 (31.01.2014)

(25) Filing Language: English

(26) Publication Language: English

(30) Priority Data:
61/819,103 3 May 2013 (03.05.2013) US

(71) Applicant: **QUANTUM VALLEY INVESTMENT FUND LP** [CA/CA]; 485 Wes Graham Way, Waterloo, Ontario N2L 0A7 (CA).

(72) Inventors: **TEKLEMARIAM, Grum**; 249 Longview Crescent, Kitchener, Ontario N2P 0A9 (CA). **CORY, David G.**; 1255 Lockie Rd., Branchton, Ontario N0B 1L0 (CA).

(74) Agent: **CLARIZIO, Dino P.**; Goodmans LLP, Bay Adelaide Centre, 333 Bay Street, Suite 3400, Toronto, Ontario M5H 2S7 (CA).

(81) Designated States *(unless otherwise indicated, for every kind of national protection available)*: AE, AG, AL, AM, AO, AT, AU, AZ, BA, BB, BG, BH, BN, BR, BW, BY, BZ, CA, CH, CL, CN, CO, CR, CU, CZ, DE, DK, DM, DO, DZ, EC, EE, EG, ES, FI, GB, GD, GE, GH, GM, GT, HN, HR, HU, ID, IL, IN, IR, IS, JP, KE, KG, KN, KP, KR, KZ, LA, LC, LK, LR, LS, LT, LU, LY, MA, MD, ME, MG, MK, MN, MW, MX, MY, MZ, NA, NG, NI, NO, NZ, OM, PA, PE, PG, PH, PL, PT, QA, RO, RS, RU, RW, SA, SC, SD, SE, SG, SK, SL, SM, ST, SV, SY, TH, TJ, TM, TN, TR, TT, TZ, UA, UG, US, UZ, VC, VN, ZA, ZM, ZW.

(84) Designated States *(unless otherwise indicated, for every kind of regional protection available)*: ARIPO (BW, GH, GM, KE, LR, LS, MW, MZ, NA, RW, SD, SL, SZ, TZ, UG, ZM, ZW), Eurasian (AM, AZ, BY, KG, KZ, RU, TJ, TM), European (AL, AT, BE, BG, CH, CY, CZ, DE, DK, EE, ES, FI, FR, GB, GR, HR, HU, IE, IS, IT, LT, LU, LV,

[Continued on next page]

(54) Title: POLARIZING A SPIN ENSEMBLE FOR MAGNETIC RESONANCE IMAGING

(57) Abstract: In some aspects, polarization of a spin ensemble can be increased using cavity-based techniques. A magnetic resonance imaging (MRI) system includes a cavity and a resonator. The cavity is adapted to interact with a spin ensemble in an imaging subject in a static magnetic field. The resonator is adapted to generate an interaction between the cavity and the spin ensemble that increases polarization of the spin ensemble. In some implementations, the spin ensemble achieves a polarization that is higher than its thermal equilibrium polarization.

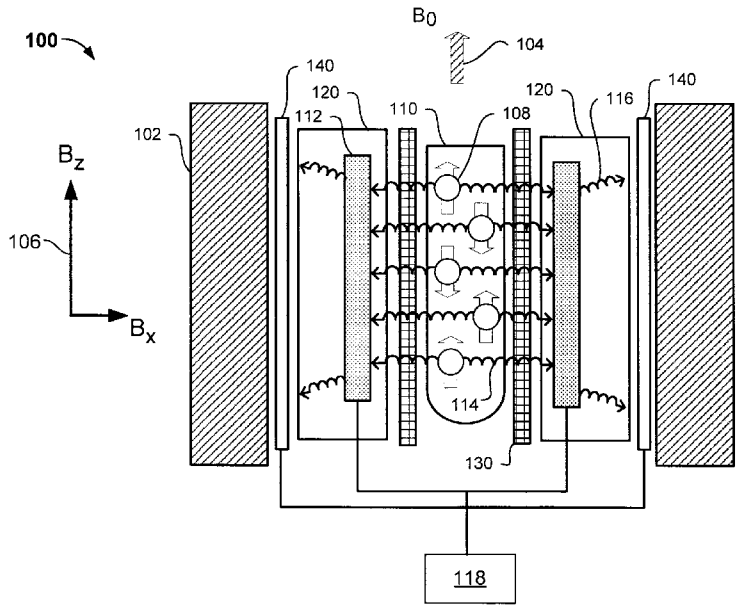


FIG. 1A

WO 2014/176663 A1

MC, MK, MT, NL, NO, PL, PT, RO, RS, SE, SI, SK, SM, TR), OAPI (BF, BJ, CF, CG, CI, CM, GA, GN, GQ, GW, KM, ML, MR, NE, SN, TD, TG).

Published:

— *with international search report (Art. 21(3))*

POLARIZING A SPIN ENSEMBLE FOR MAGNETIC RESONANCE IMAGING

CLAIM OF PRIORITY

[0001] This application claims priority to U.S. Provisional Patent Application Serial No. 61/819,103, filed on May 3, 2013, the entire contents of which are hereby incorporated by reference.

BACKGROUND

[0002] This document relates to using a cavity to polarize a spin ensemble for magnetic resonance imaging (MRI).

[0003] In magnetic resonance systems, signal-to-noise ratio (SNR) generally depends on the spin polarization and the time required to reach thermal equilibrium with the environment. The time required to reach thermal equilibrium – characterized by the energy relaxation time T_1 – often becomes long, for example, at low temperatures. Conventional techniques for removing entropy from a quantum system include dynamic nuclear polarization (DNP), algorithmic cooling, optical pumping, laser cooling, and microwave cooling, among others.

[0004] Various approaches have been used to increase the signal-to-noise ratio (SNR) in magnetic resonance applications. For instance, signal averaging over multiple acquisitions is often used to increase SNR. Another approach is to increase the induction probe sensitivity, for example, by overlapping multiple induction coils and using phased array techniques. In some systems, induction probes are embedded in cryogens to reduce intrinsic noise within the induction probes.

SUMMARY

[0005] In some aspects, a magnetic resonance imaging (MRI) system includes a cavity and a resonator. The cavity is adapted to interact with a spin ensemble in an imaging subject in a static magnetic field. The resonator is adapted to generate an interaction between the cavity and the spin ensemble that increases polarization of the spin ensemble.

[0006] In some implementations, the interaction can increase the spin ensemble's polarization faster than an incoherent thermal process (e.g., thermal spin-lattice relaxation, spontaneous emission, etc.) affecting the spin ensemble. In some implementations, the spin ensemble achieves a polarization that is higher than the thermal equilibrium polarization.

Increasing the spin ensemble's polarization may lead to an improved SNR, or other advantages in some cases.

[0007] The details of one or more implementations are set forth in the accompanying drawings and the description below. Other features, objects, and advantages will be apparent from the description and drawings, and from the claims.

DESCRIPTION OF DRAWINGS

[0008] FIG. 1A is a schematic diagram of an example magnetic resonance system.

[0009] FIG. 1B is a schematic diagram of an example control system.

[0010] FIG. 1C is a flow chart of an example technique for increasing polarization of a spin ensemble.

[0011] FIG. 2 is a plot showing a spin-resonance frequency, a cavity-resonance frequency, and a Rabi frequency in an example magnetic resonance system.

[0012] FIG. 3 shows two example energy level diagrams for a spin coupled to a two-level cavity.

[0013] FIG. 4 is a plot showing simulated evolution of the normalized expectation value of $-\langle J_x(t)\rangle/J$ for the Dicke subspace of an example cavity-cooled spin ensemble.

[0014] FIG. 5 is an energy level diagram of an example spin system coupled to a two-level cavity.

[0015] FIG. 6 is a diagram of an example 3-spin Hilbert space.

[0016] FIG. 7 is a plot showing effective cooling times calculated for example spin ensembles.

[0017] FIG. 8A is a schematic diagram showing entropy flow in an example cavity-based cooling process.

[0018] FIG. 8B is a plot showing example values of the rates Γ_{SC} and Γ_{CF} shown in FIG. 8A.

[0019] FIG. 9 is a schematic diagram of an example magnetic resonance imaging system.

[0020] Like reference symbols in the various drawings indicate like elements.

DETAILED DESCRIPTION

[0021] Here we describe techniques that can be used, for example, to increase the signal-to-noise ratio (SNR) in a magnetic resonance system by rapidly polarizing a spin ensemble. The techniques we describe can be used to achieve these and other advantages in a variety of contexts, including nuclear magnetic resonance (NMR) spectroscopy, electron spin resonance (ESR) spectroscopy, nuclear quadrupole resonance (NQR) spectroscopy, magnetic resonance imaging (MRI), quantum technologies and devices, and other applications.

[0022] We describe cavity-based cooling techniques applied to ensemble spin systems in a magnetic resonance environment. In some implementations, a cavity having a low mode volume and a high quality factor is used to actively drive all coupled angular momentum subspaces of an ensemble spin system to a state with purity equal to that of the cavity on a timescale related to the cavity parameter. In some instances, by alternating cavity-based cooling with a mixing of the angular momentum subspaces, the spin ensemble will approach the purity of the cavity in a timescale that can be significantly shorter than the characteristic thermal relaxation time of the spins (T_1). In some cases, the increase in the spin ensemble's polarization over time during the cavity-based cooling process can be modeled analogously to the thermal spin-lattice relaxation process, with an effective polarization rate $(1/T_{1,\,\mathrm{eff}})$ that is faster than the thermal relaxation rate $(1/T_1)$.

[0023] In some instances, the cavity-based cooling techniques described here can be used to increase the signal-to-noise ratio (SNR) in magnetic resonance applications. For example, the cavity-based cooling technique can provide improved SNR by increasing the polarization of the magnetic resonance sample. This SNR enhancement can be used, for example, in magnetic resonance imaging (MRI) and liquid-state magnetic resonance applications where the induction signals generated by spins are generally weak. The polarization increase and corresponding SNR improvement can be used in other applications as well.

[0024] Accordingly, the cavity can be used to remove heat from the spin ensemble (reducing the spin temperature) or to add heat to the spin ensemble (increasing the spin temperature), thereby increasing the spin polarization. Heating the spin ensemble can create an inverted polarization, which may correspond to a negative spin temperature.

[0025] FIG. 1A is a schematic diagram of an example magnetic resonance system 100. The example magnetic resonance system 100 shown in FIG. 1A includes a primary magnet system 102, a cooling system 120, a resonator and cavity system 112, a sample 110 that

contains spins 108, a control system 118, a temperature control system 130, and a gradient system 140. A magnetic resonance system may include additional or different features, and the components of a magnetic resonance system can be arranged as shown in FIG. 1A or in another manner.

[0026] In the example shown in FIG. 1A, the sample 110 is maintained at a sample temperature (T_S). In some implementations, the sample temperature (T_S) is an ambient temperature. The temperature control system 130 can provide thermal regulation that maintains the sample 110 at a specified temperature. Generally, the sample 110 can be held at any thermal temperature. In some examples, the sample 110 is a liquid or liquid-crystal material, and the sample temperature (T_S) is held at an appropriate level to maintain the sample 110 in a liquid state. In some examples, the sample 110 is a live imaging subject (e.g., a human or another type of live subject), and the sample temperature (T_S) is held at an appropriate level to maintain a desired environment for the imaging subject. The temperature control system 130 can use active or passive temperature control techniques. For example, the temperature control system 130 may use a controlled air flow about the sample 110, a heating or cooling element about the sample 110, an insulator element about the sample 110, or a combination of these and other features to control the temperature of the sample 110.

[0027] In some implementations, the temperature control system 130 includes a sample temperature controller (STC) unit. The STC unit can include a temperature regulator system that actively monitors the temperature of the sample 110 and applies temperature regulation. The temperature of the sample 110 can be monitored, for example, using a thermocouple to sense the sample temperature. The monitored temperature information can be used with a feedback system to regulate the sample temperature, for example, holding the sample temperature at a specified constant value. In some cases, the feedback system can adjust hot or cold air supplied to the sample environment by an air supply system. For example, the air supply system can include a fan that communicates heated or chilled air into the sample environment in response to control data provided by the feedback system.

[0028] The example resonator and cavity system 112 can be used to control the spin ensemble as described in more detail below. In some cases, the cavity and resonator system 112 increases polarization of the spin ensemble by heating or cooling the spin ensemble.

[0029] The cooling system 120 provides a thermal environment for the resonator and cavity system 112. In some cases, the cooling system 120 can absorb heat from the cavity to

maintain a low temperature of the cavity. In the example shown in FIG. 1A, the cooling system 120 resides in thermal contact with the resonator and cavity system 112. In some cases, the cooling system 120 maintains the resonator and cavity system 112 at liquid helium temperatures (e.g., approximately 4 Kelvin), at liquid nitrogen temperatures (e.g., approximately 77 Kelvin), or at another cryogenic temperature (e.g., less than 100 Kelvin). In some cases, the cooling system 120 maintains the resonator and cavity system 112 at pulsed-tube refrigerator temperatures (e.g., 5 -11 Kelvin), pumped helium cryostat temperatures (e.g., 1.5 Kelvin), helium-3 fridge temperatures (e.g., 300 milliKelvin), dilution refrigerator temperatures (e.g., 15 milliKelvin), or another temperature. In some implementations, the temperature (T_C) of the resonator and cavity system 112 is held at or below 10 Kelvin or 100 Kelvin, while the sample 110 is held above a melting temperature for a material in the sample (e.g., a temperature that is above 273 Kelvin for a water-based sample).

[0030] In some cases, the resonator and the cavity are implemented as two separate structures, and both are held at the same cryogenic temperature. In some cases, the resonator and the cavity are implemented as two separate structures, and the cavity is held at a cryogenic temperature while the resonator is held at a higher temperature. In some cases, an integrated resonator/cavity system is held at a cryogenic temperature. In general, various cooling systems can be used, and the features of the cooling system 120 can be adapted for a desired operating temperature T_C, for parameters of the resonator and cavity system 112, or for other aspects of the magnetic resonance system 100.

[0031] In some cases, the magnetic resonance system 100 includes one or more thermal barriers that thermally insulate the sample 110 from thermal interactions with the colder system components (e.g., components of the cooling system 120, components of the resonator and cavity system 112, etc.). For instance, the thermal barrier can prevent direct contact between the sample 110 and the cooling system 120, and the thermal barrier can be adapted to reduce indirect heat transfer between the sample 110 and the cooling system 120. For example, the temperature control system 130 can include an insulator that insulates the sample 110 against thermal interaction with the cooling system 120. In some implementations, the sample 110 can be surrounded (e.g., partially or fully surrounded) by a thermal-insulator material that has low magnetic susceptibility or is otherwise suited to magnetic resonance applications. For example, polymide-based plastic materials (e.g., VESPEL® manufactured by DUPONT™) can be used as a thermal barrier between the

sample 110 and colder system components (e.g., the cooling system 120, the resonator and cavity system 112, etc.).

[0032] In general, various cooling systems can be used, and the features of the cooling system 120 can be adapted for a desired operating temperature T_C, for parameters of the resonator and cavity system 112, or for other aspects of the magnetic resonance system 100. In the example shown in FIG. 1A, the cooling system 120 encloses the resonator and cavity system 112 and maintains the temperature T_C of the resonator and cavity system 112 below the temperature T_S of sample 110.

[0033] In some implementations, the resonator and cavity system 112 operates at a desired operating temperature T_C that is in the range from room temperature (approximately 300 K) to liquid helium temperature (approximately 4 K), and the cooling system 120 uses liquid-flow cryostats to maintain the desired operating temperature T_C. The cooling system 120 can include an evacuated cryostat, and the resonator and cavity system 112 can be mounted on a cold plate inside the cryostat. The resonator and cavity system 112 can be mounted in thermal contact with the cryostat, and it can be surrounded by a thermal radiation shield. The cooling system 120 can be connected to a liquid cryogen source (e.g., a liquid nitrogen or liquid helium Dewar) by a transfer line, through which the liquid cryogen can be continuously transferred to the cold head. The flow rate and liquid cryogen used can control the operating temperature. Gases can be vented through a vent.

[0034] In some cases, the cooling system 120 uses a closed-loop system (e.g., a commercial Gifford-McMahon pulsed-tube cryo-cooler) to maintain the desired operating temperature T_C of the resonator and cavity system 112. A closed-loop or pulsed-tube system may, in some instances, avoid the need for continuously transferring costly liquid cryogen. In some closed-loop refrigerators, the cryostat has two-stages: the first stage (ranging, e.g., from 40 to 80 K) acts as a thermal insulator for the second stage, and the second stage encases the cold head and the resonator and cavity system 112. Some example closed-loop systems can reach a stable operating temperature of 10 Kelvin.

[0035] In some cases, the cooling system 120 uses a liquid helium cryostat to maintain the desired operating temperature T_C of the resonator and cavity system 112. A liquid helium cryostat can be less complicated and more stable in some applications. When a liquid helium cryostat is used the resonator and cavity system 112 can be immersed (e.g., fully or partially immersed) in liquid helium. The system can include an outer Dewar that contains liquid

nitrogen and an inner Dewar that contains liquid helium, and the two Dewars can be separated by a vacuum jacket or another thermal insulator. Liquid helium cryostat systems can typically reach a stable operating temperature of approximately 4 Kelvin.

[0036] In some cases, the cooling system 120 uses a helium-gas-flow (or pumped-helium) cryostat to maintain the desired operating temperature T_C of the resonator and cavity system 112. Some commercial helium-gas-flow (or pumped-helium) cryostats can reach a stable operating temperature of 1.5 Kelvin. In such cases, the resonator and cavity system 112 can be mounted inside the cryostat, and a flow of helium gas can be communicated over the surface of the resonator and cavity system 112. In some implementations, the cooling system 120 includes a liquid helium Dewar that surrounds the resonator and cavity system 112 and is thermally isolated by a vacuum jacket, and a valve (e.g., a mechanically-controlled needle valve in the liquid helium Dewar) can control the flow of helium from the Dewar. The valve can control a port that opens into a gas heater, so that the liquid helium is vaporized and flows to the resonator and cavity system 112. The valve and heater can be externally controlled to provide the desired temperature regulation.

[0037] Some example helium-gas-flow cryostats can reach operating temperatures of 1 Kelvin by lowering the vapor pressure of the helium gas in the cryostat. This can be achieved by pumping on the helium in a small container (known as the "1-K pot") inside the vessel to lower the vapor pressure and thereby lower the boiling point of liquid helium (e.g., from 4.2 Kelvin down to 1 Kelvin). Some systems can cool down even further and reach milliKelvin temperatures, for example, using the helium-3 isotope (which is generally more expensive than the helium-4 isotope). The helium-3 can be pumped to much lower vapor pressures, thereby lowering the boiling point as low as 200 milliKelvin. A closed-loop system can be used to avoid leaks and preserve the helium-3 material.

[0038] In some cases, the cooling system 120 uses a dilution refrigerator system to maintain the desired operating temperature T_C of the resonator and cavity system 112. Dilution refrigerator systems typically use a helium-3 circulation system that is similar to the helium-gas-flow cryostat described above. The dilution fridge system can pre-cool the helium-3 before entering the 1-K pot, to provide an operating temperature as low as 2 milliKelvin.

[0039] The magnetic resonance system 100 shown in FIG. 1A can polarize the spin ensemble in the sample 110. For example, the magnetic resonance system 100 can cool or map the spin ensemble to a thermal equilibrium state or to another state (i.e., a state other than the thermal

equilibrium state, which may be more polarized or less polarized than the thermal equilibrium state). In some cases, the cavity-based cooling technique polarizes the spin ensemble to an extent that is determined at least partially by the temperature (T_C) of the resonator and cavity system 112.

[0040] In the example shown, the spins 108 in the sample 110 interact independently with the primary magnet system 102 and the resonator and cavity system 112. The primary magnet system 102 quantizes the spin states and sets the Larmor frequency of the spin ensemble. Rotation of the spin magnetization can be achieved, for example, by a radio-frequency magnetic field generated by a resonator. While the spins are weakly coupled to the environment, the cavity is well coupled to the environment (e.g., the cooling system 120) so that the time it takes for the cavity to reach thermal equilibrium is much shorter than the time it takes the spins to reach thermal equilibrium. The resonator can drive Rabi oscillations in the spin ensemble so that they couple to the cavity, and the Dicke states and other angular momenta subspaces of the spin system reach thermal equilibrium with the cavity.

[0041] The resonator and cavity system 112 can be described in terms of a cavity resonance and a spin resonance. The spin resonance is shifted from the cavity resonance by the Rabi frequency. The Rabi frequency (i.e., the frequency of the Rabi oscillations) can be a function of the power of the drive field applied at the spin-resonance frequency. The Rabi frequency can be configured to couple the spins to the cavity modes. For example, the power of the drive field can be set such that the Rabi frequency is substantially equal to the difference between the cavity resonance and the spin resonance. In some cases, the system can be modeled as a set of Dicke states and angular momenta subspaces of the spin ensemble (i.e., states in the Dicke and angular momenta subspace) coupled to the cavity modes through the Tavis-Cummings Hamiltonian.

[0042] A cavity having a low mode volume and high quality factor can produce a strong spin-cavity coupling for the spin ensemble. In some instances, the rate of photon exchange between the Dicke states and cavity scales as $\sqrt{N_s}$ (the number of spins in the spin ensemble) and g (the spin-cavity coupling strength for a single spin). In some examples, the spin-cavity coupling strength is inversely proportional to the square root of the mode volume and directly proportional to the square root of the admittance (i.e., the quality factor of the cavity).

[0043] In some implementations, the cavity is cooled efficiently and quickly, and the heat capacity of the cavity is large compared to the heat capacity of the spins. In some instances,

the polarization rate produced by the spin-cavity interaction can be significantly faster than the thermal T_1 relaxation process. In some cases, the polarization rate produced by the spin-cavity interaction is faster than any internal relaxation process affecting the spin ensemble, including spontaneous emission, stimulated emission, thermal T_1 relaxation, or others. For example, as a result of the low mode volume and high quality factor cavity, the efficient cavity cooling, the efficient spin-cavity coupling, the mixing of angular momenta subspaces or a combination of these and other features, the spin ensemble can be cooled quickly toward the ground state. The mixing of angular momenta subspaces can be achieved, for example, by repeating a cavity-cooling process and using an interaction such as the Dipolar coupling, natural T_2 relaxation, external gradient fields, etc. In some aspects, this can provide an effective "short circuit" of the T_1 relaxation process. For example, the technique shown in FIG. 1C can be used to achieve faster spin polarization in some instances. In some cases, as a result of the lower temperature of the cavity (compared to the higher temperature of the sample), the spin ensemble also reaches a polarization that exceeds the thermal equilibrium polarization. Accordingly, in some cases, the cavity can increase the polarization at a rate that is faster than the thermal T_1 relaxation process, and the cavity can produce a higher degree of polarization than the thermal T_1 relaxation process produces.

[0044] FIG. 1C is a flow chart showing an example process 195 for increasing polarization of a spin ensemble. The example process 195 can be performed, for example, in the example magnetic resonance system 100 shown in FIG. 1A or in another type of system. The example process 195 shown in FIG. 1C can include additional or different operations. In some cases, individual operations can be divided into multiple sub-operations, or two or more of the operations can be combined or performed concurrently as a single operation. Moreover, some or all of the operations can be iterated or repeated, for example, until a desired state or polarization is achieved or until a terminating condition is reached.

[0045] As shown in FIG. 1C, at 196, angular momenta subspaces of a spin ensemble are mapped to a lower-energy state. For example, one or more angular momenta subspaces may be cooled to their respective lowest states. In some cases, a coherent interaction between the cavity and the spin ensemble can drive each angular momentum subspace to its lowest energy state. The mapping can be generated, for example, by applying a drive field to the spin ensemble. At 197, the angular momenta subspaces are connected. One or more of a number of different techniques can be used to connect the angular momenta subspaces. In some instances, the angular momenta subspaces are connected by a process that mixes the various

subspaces of the overall space. For example, a dipolar interaction among spins, transverse (T_2) relaxation, an external gradient field, a similar external or internal dephasing interaction, or a combination of one or more of these can be used to connect the angular momenta subspaces. At 198, a more highly-polarized state is obtained. That is to say, the state of the spin ensemble can be more highly polarized than before the spin ensemble's angular momenta subspaces were cooled to their respective lowest states (at 196) and connected (at 197). The operations (196, 197) can be iterated one or more times, for example, until a desired polarization or other condition is reached.

[0046] In some implementations, the initial state of the spin ensemble (before 196) has less polarization than the spin ensemble's thermal equilibrium state. For example, the initial state of the spin ensemble may be a highly mixed state that has little or no polarization. The polarization of the state produced on each iteration can be higher than the polarization of the initial state. In some instances, the polarization is subsequently increased on each iteration. For example, the operations (196, 197) may be repeated until the spin ensemble reaches a thermal equilibrium polarization or another specified polarization level (e.g., an input polarization for a magnetic resonance sequence to be applied to the spin ensemble).

[0047] In some implementations, the process 195 can be used to polarize a spin ensemble on-demand. For example, the process 195 can be initiated at any time while the sample is positioned in the magnetic resonance system. In some cases, the spin ensemble is polarized between imaging scans or between signal acquisitions. Generally, the spin ensemble can be in any state (e.g., any fully or partially mixed state) when the process 195 is initiated. In some cases, the process 195 is initiated on-demand at a specified time, for example, in a pulse sequence, a spectroscopy or imaging process, or another process, by applying the Rabi field for a specified amount time.

[0048] In the example shown in FIG. 1A, the spin ensemble can be any collection of particles having non-zero spin that interact magnetically with the applied fields of the magnetic resonance system 100. For example, the spin ensemble can include nuclear spins, electron spins, or a combination of nuclear and electron spins. Examples of nuclear spins include hydrogen nuclei (^{1}H), carbon-13 nuclei (^{13}C), and others. In some implementations, the spin ensemble is a collection of identical spin-1/2 particles.

[0049] The example primary magnet system 102 generates a static, uniform magnetic field, labeled in FIG. 1A and referred here to as the B_0 field 104. The example primary magnet

system 102 shown in FIG. 1A can be implemented as a superconducting solenoid, an electromagnet, a permanent magnet or another type of magnet that generates a static magnetic field. In FIG. 1A, the example B_0 field 104 is homogeneous over the volume of the sample 110 and oriented along the z direction (also referred to here as the "axial direction") of the axisymmetric reference system 106.

[0050] In some instances, the gradient system 140 generates one or more gradient fields. The gradient fields are magnetic fields that spatially vary over the sample volume. In some cases, the gradient system 140 includes multiple independent gradient coils that can generate gradient fields that vary along different spatial dimensions of the sample 110. For example, the gradient system 140 can generate a gradient field that varies linearly along the z-axis, the y-axis, the x-axis, or another axis. In some cases, the gradient system 140 temporally varies the gradient fields. For example, the control system 118 can control the gradient system 140 to produce gradient fields that vary over time and space according to an imaging algorithm or pulse program.

[0051] In the example system shown in FIG. 1A, interaction between the spins 108 and the primary magnet system 102 includes the Zeeman Hamiltonian $H = -\boldsymbol{\mu} \cdot \boldsymbol{B}$, where $\boldsymbol{\mu}$ represents the magnetic moment of the spin and $\boldsymbol{B}$ represents the magnetic field. For a spin-1/2 particle, there are two states: the state where the spin is aligned with the B_0 field 104, and the state where the spin is anti-aligned with the B_0 field 104. With the B_0 field 104 oriented along the z-axis, the Zeeman Hamiltonian can be written $H = -\mu_z B_0$. Quantum mechanically, $\mu_z = \gamma\sigma_Z$ where γ is the spin gyromagnetic ratio and σ_z is the z-direction spin angular momentum operator with angular momentum eigenstates $|m\rangle_s$ and eignevalues $m = \pm 1/2\hbar$, where $\hbar$ is Planck's constant.. The factor $\omega_S = \gamma B_0$ is the spin-resonance frequency also known as the Larmor frequency.

[0052] In the example shown in FIG. 1A, the thermal distribution of individual members of the ensemble being either aligned or anti-aligned with the B_0 field 104 is governed by Maxwell-Boltzmann statistics, and the density matrix for the thermal equilibrium state is given by

$$\rho = \frac{1}{Z} e^{-H/kT},$$

where the denominator Z is the partition function, and H is the Hamiltonian of the spin ensemble. The partition function can be expressed $Z = \sum e^{-H/kT}$, where the sum is over all

possible spin ensemble configurations. The constant k is the Boltzmann factor and T is the ambient temperature. As such, the thermal equilibrium state of the spin ensemble (and the associated thermal equilibrium polarization) can be determined at least partially by the sample environment (including the magnetic field strength and the sample temperature), according to the equation above. The polarization of the spin ensemble can be computed, for example, from the density matrix representing the state of the spin ensemble. In some instances, the spin polarization in the z-direction can be computed as the expectation value of the magnetization in the z-direction, M_Z, as follows:

$$\langle M_Z \rangle = (\gamma\hbar) Tr\{J_Z \rho\}$$

where $J_Z \equiv \sum_{j=1}^{N_S} \sigma_Z^{(j)}/2$ is the total spin ensemble z-angular momentum and N_S is the ensemble spin size.

[0053] Once the spin ensemble has thermalized with its environment, any excitations that cause deviations away from thermal equilibrium will naturally take time (characterized by the thermal relaxation rate T_1) to thermalize. The thermal relaxation process evolves the spin ensemble from a non-thermal state toward the thermal equilibrium state at an exponential rate that is proportional to $1/T_1$. Many magnetic resonance applications manipulate the spins and acquire the inductive signals generated by them. Signal averaging is customarily used to improve the signal-to-noise ratio (SNR). However, the thermal relaxation process takes time, and the polarization produced by the thermal relaxation process is limited by the sample environment (including the thermal temperature of the sample and the primary magnetic field strength). In the example shown in FIG. 1A, the resonator and cavity system 112 can be used (e.g., in the example process 195 shown in FIG. 1C, or in another manner) to map the spin ensemble to a state that is more polarized than the thermal equilibrium state, and in some cases, the resonator and cavity system 112 increases the spin ensemble's polarization faster than the thermal relaxation process.

[0054] In some instances, the resonator and cavity system 112 can include a resonator component that controls the spin ensemble, and a cavity component that cools the spin ensemble. The resonator and cavity can be implemented as separate structures, or an integrated resonator/cavity system can be used. In some implementations, the resonator is tuned to a resonance frequency of one or more of the spins 108 in the sample 110. For example, the resonator can be a radio-frequency resonator, a microwave resonator, or another type of resonator.

[0055] The resonator and cavity system 112 is an example of a multi-mode resonance system. In some examples, a multi-mode resonance system has one or more drive frequencies, one or more cavity modes, and possibly other resonance frequencies or modes. The drive frequency can be tuned to the spins' resonance frequency, which is determined by the strength of the B_0 field 104 and the gyromagnetic ratio of the spins 108; the cavity mode can be shifted from the drive frequency. In some multi-mode resonance systems, the drive frequency and the cavity mode are provided by a single integrated structure. Examples of integrated multi-mode resonator structures include double-loop resonators, birdcage resonators, and other types of structures. In some multi-mode resonance systems, the drive frequency and cavity mode are provided by distinct structures. In some cases, the geometry of a low quality factor (low-Q) coil can be integrated with a high-Q cavity such that both the coil and cavity are coupled to the spin system but not to each other. The techniques described here can operate using a single drive frequency or possibly multiple drive frequencies applied to the coil.

[0056] In the example shown in FIG. 1A, the cavity has a resonance frequency ω_c that is different from the resonance frequency of the resonator. The cavity of the example resonator and cavity system 112 supports electromagnetic waves whose modes are determined by physical characteristics of the cavity. Typically, the fundamental mode is used as the cavity resonance and the quality factor of the cavity (Q) can be defined as the ratio of the stored energy in the cavity mode to the dissipated energy. In terms of frequency units, the quality factor of the cavity may be represented

$$Q = \frac{\omega_c}{\Delta\omega},$$

where ω_c is the cavity-resonance frequency, and $\Delta\omega$ is the -3 dB bandwidth of the cavity resonance. In cases where the cavity resonance is given by a distribution that is Lorentzian, the bandwidth is given by the full-width at half-maximum (FWHM) of the cavity frequency response.

[0057] In some implementations, the cavity of the example resonator and cavity system 112 has a high quality factor (a high-Q cavity), so that an electromagnetic field in the cavity will be reflected many times before it dissipates. Equivalently, the photons in the cavity have a long lifetime characterized by the cavity dissipation rate $\kappa = (\omega/Q)$, where ω is the frequency of the wave. Such cavities can be made of superconducting material and kept at cryogenic temperatures to achieve quality factors that are high in value. For example, the

quality factor of a high-Q cavity can have an order of magnitude in the range of $10^3 - 10^6$ or higher. Under these conditions, the electromagnetic field in the cavity can be described quantum mechanically as being equivalent to a quantum harmonic oscillator: a standard treatment known as cavity quantum electrodynamics or cavity QED. This treatment of the electromagnetic field in the cavity is in contrast to the Zeeman interaction where only the spin degree of freedom is quantum mechanical while the magnetic field is still classical.

[0058] For purposes of illustration, here we provide a quantum mechanical description of the cavity modes. Electromagnetic waves satisfy Maxwell's equations and both the electric field **E** and the magnetic field **B** can be described in terms of a vector potential **A** as

$$\mathbf{B} = \nabla \times \mathbf{A},$$

$$\mathbf{E} = \frac{\partial \mathbf{A}}{\partial t}.$$

The vector potential itself satisfies the wave equation

$$\nabla^2 \boldsymbol{A} = \frac{1}{c^2}\frac{\partial^2 \boldsymbol{A}}{\partial t^2},$$

where c is the speed of light. The wave equation has a formal solution in the form of the Fourier series of plane waves:

$$A = \sum_k (\boldsymbol{A}_k(t)\, e^{i\boldsymbol{k}.\boldsymbol{r}} + \boldsymbol{A}_k^*(t)\, e^{-i\boldsymbol{k}.\boldsymbol{r}}),$$

where each Fourier component $\boldsymbol{A}_k(t)$ also satisfies the wave equation. These plane waves are ones that the cavity supports in the case of cavity QED and by assuming $\boldsymbol{A}_k(t)$ has time-dependence of the form $\boldsymbol{A}_k(t) = \boldsymbol{A}_k\, e^{i\omega_k t}$, the electric and magnetic fields are given by

$$\boldsymbol{E}_k = i\omega_k\left(\boldsymbol{A}_k\, e^{-i\omega_k t + i\boldsymbol{k}.\boldsymbol{r}} - \boldsymbol{A}_k^*\, e^{i\omega_k t - i\boldsymbol{k}.\boldsymbol{r}}\right),$$

$$\boldsymbol{B}_k = i\boldsymbol{k} \times \left(\boldsymbol{A}_k\, e^{-i\omega_k t + i\boldsymbol{k}.\boldsymbol{r}} - \boldsymbol{A}_k^*\, e^{i\omega_k t - i\boldsymbol{k}.\boldsymbol{r}}\right),$$

where the temporal and spatial frequencies (ω_k and k, respectively) are related by $\omega_k = ck$.

[0059] Accordingly, the energy of a single mode k is given by

$$W_k = \frac{1}{2}\int dV\, (\epsilon_0 \boldsymbol{E}_k^2 + \mu_0^{-1}\boldsymbol{B}_k^2) = 2\epsilon_0 V \omega_k^2\, \boldsymbol{A}_k.\boldsymbol{A}_k^*$$

where ϵ_0 and μ_0 are the permittivity and permeability of free space respectively, such that $c^2\mu_0\epsilon_0 = 1$ and V is the volume of space or cavity containing the radiation field. By defining the vector coefficients in terms of a real and imaginary part P and Q, we can express $\boldsymbol{A}_k$ as:

$$\boldsymbol{A}_k = (4\epsilon_0 V\omega_k^2)^{-\frac{1}{2}}(\omega_k \boldsymbol{Q}_k + i\boldsymbol{P}_k)\epsilon_k,$$

where ϵ_k is the polarization vector for the electromagnetic wave. In terms of $\boldsymbol{Q}_k$ and $\boldsymbol{P}_k$ the energy is given by

$$W_k = \frac{1}{2}(P_k^2 + \omega_k^2 Q_k^2),$$

which is the form for the energy of a simple harmonic oscillator. Hence, we may treat the vectors $\boldsymbol{Q}_k$ and $\boldsymbol{P}_k$ of the electromagnetic wave as the position and momentum vectors of the Harmonic oscillator. This allows us to quantize the electromagnetic field in terms of single quanta (photons) by the standard canonical quantization of the harmonic oscillator.

[0060] We now consider the quantum treatment of a single electromagnetic mode in a cavity. The Hamiltonian for the quantum harmonic oscillator may be written in terms of the canonical P and Q variables as

$$H = \frac{1}{2}(P^2 + \omega^2 Q^2).$$

We may then define operators a and a^+, called the annihilation and creation operators, respectively, in terms of the vectors P and Q:

$$a = \sqrt{\frac{\omega}{2\hbar}}\left(Q + \frac{i}{\omega}P\right),$$

$$a^+ = \sqrt{\frac{\omega}{2\hbar}}\left(Q - \frac{i}{\omega}P\right).$$

These operators satisfy the commutation relation $[a, a^+] = 1$. Hence, our Hamiltonian may be written in terms of the creation and annihilation operators as

$$H = \hbar\omega\left(a^+a + \frac{1}{2}\right).$$

The constant factor of a half corresponds to a constant energy shift of the cavity modes so we may remove it by going into an interaction frame which rescales the energies by this constant amount.

[0061] The energy eigenstates of this Hamiltonian are the so-called number states, which correspond to a single quanta (photon) of radiation within the cavity. They are labeled $|n\rangle_c$ where $n = [0, 1, 2, 3, \ldots]$. The action of the creation and annihilation operators on the number states is to create or remove a photon from the cavity:

$$a|n\rangle_c = \sqrt{n}|n-1\rangle_c$$

$$a^+|n\rangle_c = \sqrt{n+1}|n+1\rangle_c$$

Hence the operator $N = a^+a$ (the number operator) gives the total number of photons for a given number state:

$$a^+a|n\rangle_c = n|n\rangle_c.$$

The photon number state $|n\rangle_c$ is an energy eigenstate of the Hamiltonian

$$H|n\rangle = \hbar\omega\left(n + \frac{1}{2}\right)|n\rangle_c,$$

with energy $\left(n + \frac{1}{2}\right)\hbar\omega$.

[0062] We now describe how the cavity of the example resonator and cavity system 112 couples to the spin ensemble containing the spins 108. The dominant interaction is once again the spin magnetic dipole coupling to the cavity electromagnetic fields. Therefore, we have

$$H_I = -\boldsymbol{\mu} \cdot \boldsymbol{B},$$

and now the electromagnetic field of the cavity is treated quantum mechanically. In terms of the harmonic oscillator operators the magnetic field in the cavity can be written as

$$\boldsymbol{B}(\boldsymbol{r}, t) = \sqrt{\frac{\mu_0\hbar\omega}{2V}}(a - a^\dagger)u(\boldsymbol{r}, t)\boldsymbol{\epsilon}$$

where $\boldsymbol{\epsilon}$ is the propagation direction, μ_0 is the free space permeability constant, $\hbar$ is the Planck constant, and the function $u(\boldsymbol{r}, t)$ represents the spatial and temporal wave behavior. For some examples, we take $\boldsymbol{\epsilon} = \hat{\boldsymbol{x}}$, and the function $u(\boldsymbol{r}, t)$ takes the form

$$u(\boldsymbol{r}, t) = u(\boldsymbol{r})\cos\omega t = u(y, z)\cos kx \cos\omega t,$$

where $u(y, z)$ represents the cavity magnetic field spatial profile. In this form, the mode volume can be expressed

$$V = \frac{\int |u(\boldsymbol{r})|^2 d^3\boldsymbol{r}}{max[|u(\boldsymbol{r})|^2]}.$$

As such, the mode volume is related to the spatial profile of the cavity magnetic field, and higher spatial homogeneity in the cavity magnetic field generally produces a lower mode volume. The spin-cavity interaction Hamiltonian then becomes

$$H_I = \frac{1}{2} g\hbar(a - a^\dagger)\sigma_x,$$

where the constant g represents the coupling strength between each spin and the cavity, and σ_x is the x-component spin angular momentum operator. The coupling strength can, in some instances, be defined by the expression

$$g\hbar = -\boldsymbol{\mu} \cdot |\langle 0|\boldsymbol{B}|1\rangle| = \sqrt{\frac{\mu_0 \gamma^2 \hbar\omega}{2V}}\,|u(\boldsymbol{r})|\,.$$

In the example equations above, the spin-cavity coupling strength is inversely proportional to the square root of the mode volume.

[0063] The example resonator and cavity system 112 includes a resonator that can generate a Rabi field that is applied to the spin ensemble while the sample resides in the B_0 field 104. For example, the Rabi field can be a continuous field or a pulsed spin-locking field. In combination with the internal Hamiltonian of the spin system, the Rabi field can provide universal control of the spin ensemble. In some implementations, any magnetic resonance experiment or pulse sequence can be implemented in this manner. The resonator can generate the Rabi field, for example, based on signals from the control system 118, and the parameters of the field (e.g., the phase, power, frequency, duration, etc.) can be determined at least partially by the signal from the control system 118.

[0064] In the plot 200 shown in FIG. 2, the vertical axis 202 represents the frequency response of the resonator and the cavity, the horizontal axis 204 represents a range of frequencies, and the curve 206 shows the response shape for an example implementation of the resonator and cavity system 112. In the example shown, the lower frequency resonance (labeled ω_s) is that of the resonator and the higher frequency resonance (labeled ω_c) is that of the cavity. The quality factor (Q) of the cavity is higher than the quality factor (Q) of the resonator, and the resonance frequencies differ by the Rabi frequency (labeled Ω_R).

[0065] The example control system 118 can control the resonator and cavity system 112 and the gradient system 140 in the magnetic resonance system 100 shown in FIG. 1A. In some cases, the control system 118 can also control aspects of the cooling system 120, the temperature control system 130, or other components of the magnetic resonance system 100. The control system 118 is electrically coupled to, and adapted to communicate with, the resonator and cavity system 112. For example, the control system 118 can be adapted to provide a voltage or current signal that drives the resonator, the cavity, or both; the control system 118 can also acquire a voltage or current signal from the resonator, the cavity, or both.

[0066] When the sample 110 is an imaging subject, the control system 118 can combine a desired operation with gradient waveforms to generate a magnetic resonance imaging pulse sequence that manipulates the spins. The pulse sequence can be applied, for example, through operation of the resonator and cavity system 112 and the gradient system 140, to spatially encode the spin ensemble so that the received magnetic resonance signals can be processed and reconstructed into an image.

[0067] FIG. 1B is a schematic diagram of an example control system 150. The example control system 150 shown in FIG. 1B includes a controller 152, a waveform generator 154, and amplifier 156, a transmitter/receiver switch 158, a receiver 160, a signal processor 162, a gradient waveform generator 164, and gradient electronics 166. A control system can include additional or different features, and the features of a control system can be configured to operate as shown in FIG. 1B or in another manner.

[0068] In the example shown in FIG. 1B, the example control system 150 is adapted to communicate with an external system 190. For example, the external system 190 can be a resonator, a cavity, or another component of a magnetic resonance system. The control system 150 can operate based on inputs provided by one or more external sources, including the external system 190 or another external source. For example, the control system can receive input from an external computer, a human operator, or another source.

[0069] The example control system 150 shown in FIG. 1B can operate in multiple modes of operation. In a first example mode of operation, the controller 152 provides a desired control operation 170 to the waveform generator 154. Based on the desired control operation 170, the waveform generator 154 generates a waveform 172. In some cases, the waveform generator 154 also receives system model data 171, and uses the system model data 171 to generate the waveform 172. The waveform 172 is received by the amplifier 156. Based on the waveform

172, the amplifier 156 generates a transmit signal 174. In this mode of operation, the transmitter/receiver switch 158 is configured to output the transmit signal 174 to the external system 190.

[0070] In a second example mode of operation, the transmitter/receiver switch 158 is configured to acquire a signal from the external system 190. The control system 150 can amplify, process, analyze, store, or display the acquired signal. As shown in FIG. 1B, based on the signal acquired from the external system 190, the transmitter/receiver switch 158 provides a received signal 176 to the receiver 160. The receiver 160 conditions the received signal 176 and provides the conditioned signal 178 to the signal processor 162. The signal processor 162 processes the conditioned signal 178 and generates data 180. The data 180 is provided to the controller 152 for analysis, display, storage, or another action.

[0071] In these and other modes of operation, the controller 152 can also provide a desired control operation 182 to the gradient waveform generator 164. Based on the desired control operation 182 (which may be the same as, or may be related to, the desired control operation 170), the waveform generator 154 generates a gradient waveform 184. The gradient electronics 166 generate a gradient control signal 186 based on the gradient waveform 184, and the gradient control signal 186 is provided to the external system 190. In some cases, a gradient coil or another device in the external system 190 generates a gradient field based on the gradient control signal 186.

[0072] In some cases, the controller 152 includes software that specifies the desired control operations 170 and 182 so as to spatially encode a spin ensemble in an imaging subject, and the software can construct an image of the imaging subject based on the data 180 derived from the received signal 176. The spatial encoding prescription can use appropriate magnetic resonance imaging techniques (e.g., typically including a Fourier transform algorithm), and the image can be constructed from the digitized data by a corresponding decoding prescription (e.g., typically including an inverse Fourier transform algorithm).

[0073] The controller 152 can be (or include) a computer or a computer system, a digital electronic controller, a microprocessor or another type of data-processing apparatus. The controller 152 can include memory, processors, and may operate as a general-purpose computer, or the controller 152 can operate as an application-specific device.

[0074] We now show an example process by which the spin ensemble in the sample 110 can couple to the cavity and cool under a coherent Rabi drive. We start with an inductively driven

ensemble of non-interacting spin-1/2 particles (represented in FIG. 1A by the spins 108) quantized in a large static magnetic field (represented in FIG. 1A by the B_0 field 104) and magnetically coupled to a high-Q cavity of the resonator and cavity system 112. In the presence of the drive provided by the resonator of the resonator and cavity system 112, the spins interact with the cavity via coherent radiative processes and the spin-cavity system can be treated quantum mechanically as a single collected magnetic dipole coupled to the cavity. In analogy to quantum optics, we describe the spin-cavity dynamics as being generated by the Tavis-Cummings (TC) Hamiltonian. Assuming the control field to be on resonance with the Larmor frequency of the spins, the spin-cavity Hamiltonian under the rotating-wave approximation (RWA) is given by $H = H_0 + H_R(t) + H_I$, with

$$H_0 = \omega_c a^\dagger a + \omega_s J_z,$$

$$H_R(t) = \Omega_R \cos(\omega_s t) J_x, \text{ and}$$

$$H_I = g(a^\dagger J_- + a J_+).$$

As before, $a^\dagger(a)$ are the creation (annihilation) operators describing the cavity, Ω_R is the strength of the drive field (Rabi frequency), ω_c is the resonant frequency of the cavity, ω_s is the Larmor resonance frequency of the spins, and g is the coupling strength of the cavity to a single spin in the ensemble in units of $\hbar = 1$. Here we have used the notation that

$$J_\alpha \equiv \sum_{j=1}^{N_s} \sigma_\alpha^{(j)}/2$$

are the total angular momentum spin operators for an ensemble of N_s spins. The state-space V of a spin ensemble of N_s identical spins may be written as the direct sum of coupled angular momentum subspaces

$$V = \bigoplus_{J=j_0}^{\frac{N_S}{2}} V_J^{\oplus n_J}$$

where $j_0 = 0\ (1/2)$ if N_s is even (odd). V_J is the state space of a spin-J particle with dimension $d_J = 2J + 1$, and there are n_J degenerate subspaces with the same total spin J. Since the TC Hamiltonian has a global $SU(2)$ symmetry, it will not couple between subspaces in this representation. The largest subspace in this representation is called the Dicke subspace and consists of all totally symmetric states of the spin ensemble. The Dicke subspace corresponds to a system with total angular momentum $J = N_s/2$. The TC

Hamiltonian restricted to the Dicke subspace is known as the Dicke model and has been studied for quantum optics.

[0075] The eigenstates of H_0 are the tensor products of photon-number states for the cavity and spin states of collective angular momentum of each total-spin subspace in the J_z direction: $|n\rangle_c|J,m_z\rangle_s$. Here, $n = 0,1,2,...$, $m_z = -J, -J+1, ..., J-1, J$, and J indexes the coupled angular momentum subspace V_J. The collective excitation number of the joint system is given by $N_{\text{ex}} = a^\dagger a + (J_z + J)$. The interaction term H_I commutes with N_{ex}, and hence preserves the total excitation number of the system. This interaction can drive transitions between the state $|n\rangle_c|J,m_z\rangle_s$ and states $|n+1\rangle_c|J,m_z-1\rangle_s$ and $|n-1\rangle_c|J,m_z+1\rangle_s$ at a rate of $\sqrt{(n+1)(J(J+1)-m_z(m_z-1))}$ and $\sqrt{n(J(J+1)-m_z(m_z+1))}$, respectively.

[0076] After moving into a rotating frame defined by $H_1 = \omega_s(a^\dagger a + J_z)$, the spin-cavity Hamiltonian is transformed to

$$\tilde{H}^{(1)} = e^{itH_1}H_{sc}e^{-itH_1} - H_1,$$

$$\tilde{H}^{(1)} = \delta\omega a^\dagger a + \Omega_R J_x + g(a^\dagger J_- + aJ_+).$$

Here, $\delta\omega = \omega_c - \omega_s$ is the detuning of the drive from the cavity-resonance frequency, and we have made the standard rotating wave approximation (RWA) to remove any time dependent terms in the Hamiltonian.

[0077] If we now move into the interaction frame of $H_2 = \delta\omega a^\dagger a + \Omega_R J_x/2$, the Hamiltonian transforms to

$$\tilde{H}^{(2)}(t) = H_{0\Omega_R}(t) + H_{-\Omega_R}(t) + H_{+\Omega_R}(t)$$

$$H_{0\Omega_R}(t) = g\left(e^{-i\delta\omega t}a + e^{i\delta\omega t}a^\dagger\right)J_x$$

$$H_{-\Omega_R}(t) = \frac{ig}{2}\left(e^{-i(\delta\omega-\Omega_R)t}aJ_+^{(x)} - e^{i(\delta\omega-\Omega_R)t}a^\dagger J_-^{(x)}\right)$$

$$H_{+\Omega_R}(t) = \frac{ig}{2}\left(e^{-i(\delta\omega+\Omega_R)t}aJ_-^{(x)} - e^{i(\delta\omega+\Omega_R)t}a^\dagger J_+^{(x)}\right)$$

where $J_\pm^{(x)} \equiv J_y \pm iJ_z$ are the spin-ladder operators in the x-basis.

[0078] In analogy to Hartmann-Hahn matching in magnetic resonance cross-relaxation experiments for $\delta\omega > 0$, we may set the cavity detuning to be close to the Rabi frequency of the drive, so that $\Delta = \delta\omega - \Omega_R$ is small compared to $\delta\omega$. By making a second rotating-wave

approximation in the interaction Hamiltonian reduces to the $H_{-\Omega_R}$ flip-flop exchange interaction between the cavity and spins in the x-basis:

$$H_I(t) = \frac{ig}{2}\left(e^{i\Delta t}aJ_+^{(x)} - e^{-i\Delta t}a^\dagger J_-^{(x)}\right)$$

This rotating-wave approximation is valid in the regime where the detuning and Rabi drive strength are large compared to the time scale, t_c, of interest ($\delta\omega$, $\Omega_R \gg 1/t_c$). From here we will drop the (x) superscript and just note that we are working in the J_x eigenbasis for our spin ensemble.

[0079] In some implementations, isolating the spin-cavity exchange interaction allows efficient energy transfer between the two systems, permitting them to relax to a joint equilibrium state in the interaction frame of the control field. The coherent enhancement of the ensemble spin-cavity coupling can enhance spin polarization in the angular momenta subspaces V_J at a rate greatly exceeding the thermal relaxation rate. FIG. 3 shows this coherent enhancement in terms of the coupled energy levels of the spin-cavity states.

[0080] FIG. 3 shows two example energy level diagrams 302, 304 for a spin coupled to a two-level cavity. In both diagrams, the ket $|+0\rangle$ represents the ground state of the spin-cavity system (where the spin and the cavity are in their respective ground states); the ket $|-1\rangle$ represents the excited state of the spin-cavity system (where the spin and the cavity are in their respective excited states), and the kets $|+1\rangle$ and $|-0\rangle$ represent intermediate states. In FIG. 3, the straight arrows represent coherent oscillations, and the curved arrows represent cavity dissipation.

[0081] FIG. 3 shows that when the cavity detuning is matched to the Rabi drive strength, energy exchange transitions between spin and cavity are enhanced. The energy level diagram 302 on the left shows the transitions without the coherent enhancement provided by the control drive. The energy level diagram 304 on the right shows the transition with the coherent enhancement provided by the control drive when $\Delta = \delta\omega - \Omega_R$ is small compared to $\delta\omega$. As shown in the energy level diagram 302 on the left, without the control drive all transition pathways are possible. The energy level diagram 304 on the right shows that when the Rabi drive is turned on and the cavity detuning is matched to the Rabi frequency, the energy exchange transitions between the spin and cavity are enhanced.

[0082] In the description below, to model the cavity-induced cooling of the spin system, we use an open quantum system description of the cavity and spin ensemble. The joint spin-

cavity dynamics may be modeled using the time-convolutionless (TCL) master equation formalism, allowing the derivation of an effective dissipator acting on the spin ensemble alone. Since the spin-subspaces V_J are not coupled by the TC Hamiltonian, the following derivation is provided for all values of J in the state-space factorization.

[0083] The evolution of an example spin-cavity system can be described by the Lindblad master equation

$$\frac{d}{dt}\rho(t) = \mathcal{L}_I(t)\rho(t) + \mathcal{D}_c\rho(t),$$

where $\mathcal{L}_I$ is the super-operator $\mathcal{L}_I(t)\rho = -i[H_I(t), \rho]$ describing evolution under the interaction Hamiltonian and $\mathcal{D}_c$ is a dissipator describing the quality factor of the cavity phenomenologically as a photon amplitude damping channel:

$$\mathcal{D}_c = \frac{\kappa}{2}\Big((1+\bar{n})D[a] + \bar{n}D[a^\dagger]\Big).$$

Here, the function $D[A](\rho) = 2A\rho A^\dagger - \{A^\dagger A, \rho\}$, $\bar{n} = \mathrm{tr}\big[a^\dagger a \rho_{eq}\big]$ characterizes the temperature of the environment (e.g., the cooling system or other environment), and κ is the cavity dissipation rate ($\propto 1/Q$). The expectation value of the number operator at equilibrium is related to the temperature T_c of the environment by

$$\bar{n} = \left(e^{\omega_c/k_B T} - 1\right)^{-1} \Leftrightarrow T = \frac{\omega_c}{k_B}\left[\ln\left(\frac{1+\bar{n}}{\bar{n}}\right)\right]^{-1},$$

where k_B is the Boltzmann constant.

[0084] The reduced dynamics of the spin ensemble in the interaction frame of the dissipator is given to second order by the TCL master equation:

$$\frac{d}{dt}\rho_s(t) = \int_0^{t-t_0} d\tau\, \mathrm{tr}_c\big[\mathcal{L}_I(t)e^{\tau\mathcal{D}_c}\mathcal{L}_I(t-\tau)\rho_s(t)\otimes\rho_{\mathrm{eq}}\big]$$

where $\rho_s(t) = \mathrm{tr}_c[\rho(t)]$ is the reduced state of the spin ensemble and ρ_{eq} is the equilibrium state of the cavity. Under the condition that $\kappa \gg g\sqrt{N_s}$, the master equation reduces to

$$\frac{d}{dt}\rho_s(t) = \frac{g^2}{4}\int_0^{t-t_0} d\tau e^{-\kappa\tau/2}(\cos(\Delta\tau)\,\mathcal{D}_s\rho_s(t) - \sin(\Delta\tau)\mathcal{L}_s(t)\rho(t)),$$

where

$$\mathcal{D}_s = (1+\bar{n})D[J_-] + \bar{n}D[J_+],$$

$\mathcal{L}_s\rho = -i[H_s, \rho]$, and

$H_s = (1+\bar{n})\, J_+J_- - \bar{n}\, J_-J_+$

are the effective dissipator and Hamiltonian acting on the spin ensemble due to coupling with the cavity.

[0085] Under the condition that $\kappa \gg g\sqrt{N_s}$ we may take the upper limit of the integral in the equation above to infinity to obtain the Markovian master equation for the driven spin ensemble:

$$\frac{d}{dt}\rho_s(t) = \left(\Omega_s\mathcal{L}_s + \frac{\Gamma_s}{2}\mathcal{D}_s\right)\rho_s(t),$$

where

$$\Omega_s = -\frac{g^2\Delta}{\kappa^2 + 4\Delta^2}, \qquad \Gamma_s = \frac{g^2\kappa}{\kappa^2 + 4\Delta^2}.$$

Here, $\Omega_s$is the frequency of the effective Hamiltonian, and Γ_s is the effective dissipation rate of the spin-system.

[0086] We can consider the evolution of a spin state that is diagonal in the coupled angular momentum basis, $\rho(t) = \sum_J \sum_{m=-J}^{J} P_m(t)\rho_{J,m}$. Here, the sum over J is summing over subspaces V_J, and $P_{J,m}(t) = \langle J,m|\rho(t)|J,m\rangle$ is the probability of finding the system in the state $\rho_{J,m} = |J,m\rangle\langle J,m|$ at time t. In this case the Markovian master equation reduces to a rate equation for the populations:

$$\frac{d}{dt}P_{J,m}(t) = \Gamma_s\left(A_{J,m+1}P_{J,m+1}(t) + B_{J,m}P_{J,m}(t) + C_{J,m-1}P_{J,m-1}(t)\right),$$

where

$A_{J,m} = (1+\bar{n})[J(J+1) - m(m-1)]$

$C_{J,m} = \bar{n}[J(J+1) - m(m+1)]$, and

$B_{J,m} = -(A_m + C_m)$.

Defining $\vec{P}_J(t) = \left(P_{J,-J}(t), \ldots, P_{J,J}(t)\right)$, we obtain the following matrix differential equation for each subspace V_J:

$$\frac{d}{dt}\vec{P}_J(t) = \Gamma_s M_J \vec{P}_J(t),$$

where M_J is the tridiagonal matrix

$$M_J = \begin{pmatrix} B_{J,-J} & A_{J,-J+1} & 0 & 0 & 0 & \cdots & 0 \\ C_{J,-J} & B_{J,-J+1} & A_{J,-J+2} & 0 & 0 & \cdots & 0 \\ 0 & C_{J,-J+1} & B_{J,-J+2} & A_{J,-J+3} & 0 & \cdots & 0 \\ \vdots & & & \ddots & & & \vdots \\ 0 & & \cdots & & 0 & C_{J,J-1} & B_{J,J} \end{pmatrix}.$$

[0087] For a given state specified by initial populations $\vec{P}_J(0)$, the above differential equation has the solution $\vec{P}_J(t) = \exp(t\Gamma_s M_J)\,\vec{P}_J(0)$. The equilibrium state of each subspace V_J of the driven spin ensemble satisfies $M_J \cdot \vec{P}_J(\infty) = 0$, and is given by

$$\rho_{J,\,\mathrm{eq}} = \sum_{m=-J}^{J} P_{J,m}(\infty)\rho_{J,m},$$

where

$$P_{J,m}(\infty) = \frac{\bar{n}^{J+m}(1+\bar{n})^{J-m}}{(1+\bar{n})^{2J+1} - \bar{n}^{2J+1}}.$$

The total spin expectation value for the equilibrium state of the spin ensemble is

$$\langle J_x \rangle_{eq} = -J + \bar{n} - \frac{(2J+1)\bar{n}^{2J+1}}{(1+\bar{n})^{2J+1} - \bar{n}^{2J+1}}.$$

[0088] If we consider the totally symmetric Dicke subspace in the limit of $N_s \gg \bar{n}$, we have that the ground state population at equilibrium is given by $P_{N_s/2,-N_s/2} \approx 1/(1+\bar{n})$ and the final expectation value is approximately $\langle J_x \rangle_{eq} \approx -N_s/2 + \bar{n}$. Thus, the final spin polarization in the Dicke subspace will be roughly equivalent to the thermal cavity polarization.

[0089] We note that, if the detuning $\delta\omega$ were negative in the example described above, matching $\Omega_R = \delta\omega$ would result in the $H_{+\Omega_R}$ term being dominant, leading to a master equation with the operators J_- and J_+ interchanged, the dynamics of which would drive the spin ensemble towards the $\langle J_x \rangle = J$ state. The detuning can be made larger than the cavity linewidth to prevent competition between the $H_{-\Omega_R}$ and $H_{+\Omega_R}$ terms, which would drive the spin system to a high entropy thermally mixed state.

[0090] In some implementations, the cavity-resonance frequency (ω_c) is set below the spin-resonance frequency (ω_s) such that the detuning $\delta\omega = \omega_c - \omega_s$ is a negative value. In such cases, the techniques described here can be used to perform cavity-based heating of the spins

to increase the polarization of spin ensemble. In such cases, the energy of the spin ensemble is increased by the interaction between the cavity and the spin ensemble.

[0091] The tridiagonal nature of the rate matrix allows $\vec{P}_{J_j}(t) = \exp(t\Gamma_s M_j)\,\vec{P}_j(0)$ to be efficiently simulated for large numbers of spins. For simplicity we will consider the cooling of the Dicke subspace in the ideal case where the cavity is cooled to its ground state ($\bar{n} = 0$), and the spin ensemble is taken to be maximally mixed (i.e., $P_m(0) = 1/(2J+1)$ for $m = -J, \ldots, J$).

[0092] FIG. 4 is a plot 400 showing simulated evolution of the normalized expectation value of $-\langle J_x(t)\rangle/J$ for the Dicke subspace of an example cavity-cooled spin ensemble. In the plot 400, the vertical axis 402 represents a range of values of the normalized expectation value of $-\langle J_x(t)\rangle/J$ for the Dicke subspace, and the horizontal axis 404 represents a range of time values. In FIG. 4, the expectation values represented by the vertical axis 402 are normalized by $-J$ to obtain a maximum value of 1, and the time variable represented by the horizontal axis 404 is scaled by the effective dissipation rate Γ_S for the spin ensemble.

[0093] The plot 400 includes four curves; each curve represents the simulated expectation value of $\langle J_x(t)\rangle$ for the Dicke subspace of a spin ensemble with a different number of total spins N_s, ranging from $N_s = 10^2$ to $N_s = 10^5$. The curve 406a represents a spin ensemble of 10^2 spins; the curve 406b represents a spin ensemble of 10^3 spins; the curve 406c represents a spin ensemble of 10^4 spins; and the curve 406d represents a spin ensemble of 10^5 spins.

[0094] At a value of $-\langle J_x(t)\rangle/J = 1$, the total angular momentum subspace of the spin ensemble is completely polarized to the J_x ground eigenstates $|J, -J\rangle$. As shown in FIG. 4, the polarization of each spin ensemble increases over time, and the polarization increases faster for the larger spin ensembles. For the examples shown, the three larger spin ensembles are substantially fully polarized within the timescale shown in the plot 400.

[0095] In some cases, the expectation value $\langle J_x(t)\rangle$ versus time can be fitted to an exponential to derive an effective cooling time-constant, $T_{1,\,\mathrm{eff}}$, analogous to the thermal spin-lattice relaxation time T_1. A fit to a model given by

$$-\frac{\langle J_x(t)\rangle}{J} = 1 - \exp\left(-\frac{t}{T_{1,\,\mathrm{eff}}}\right)$$

yields the parameters $T_{1,\text{eff}} = \lambda(2J)^{\gamma}/\Gamma_s$ with $\lambda = 2.0406$ and $\gamma = -0.9981$. This model includes an exponential rate $(1/T_{1,\text{eff}})$, analogous to the thermal spin-lattice relaxation process, which includes an exponential rate $(1/T_1)$. This model can be used for an angular momentum subspace (e.g., the Dicke subspace) or the full Hilbert space. In some instances, the effective rate $(1/T_{1,\text{eff}})$ is significantly faster than the thermal rate $(1/T_1)$. An approximate expression for the cooling-time constant for the spin subspace V_J as a function of J is

$$T_{1,\text{eff}}(J) \approx \frac{2}{\Gamma_s J_s} = \frac{2(\kappa^2 + 4\Delta^2)}{g^2 \kappa J}.$$

In this effective cooling time-constant, the cooling efficiency is maximized when the Rabi drive strength is matched to the cavity detuning (i.e., $\Delta = 0$). In this case, the cooling rate and time-constant simplify to $\Gamma_s = g^2/\kappa$ and $T_{1,\text{eff}} = \kappa/g^2 J$, respectively. In the case where the cavity is thermally occupied, the final spin polarization is roughly equal to the thermal cavity polarization, and for cavity temperatures corresponding to $\bar{n} < \sqrt{2J}$ the effective cooling constant $T_{1,\text{eff}}$ is approximately equal to the zero temperature value.

[0096] A magnetic resonance system can be controlled in a manner that polarizes a sample at a rate corresponding to the effective cooling constant $T_{1,\text{eff}}$ shown above. The magnetic resonance system can be configured according to the parameters that adhere to the two rotating wave approximations used to isolate the spin-cavity exchange term $H_I(t)$. For implementations where $\delta\omega \approx \Omega_R$, the magnetic resonance system can be configured such that $g\sqrt{N_s} \ll \kappa \ll \Omega_R, \delta\omega \ll \omega_c, \omega_s$.

[0097] For an example implementation using X-band pulsed electron spin resonance (ESR) ($\omega_c/2\pi \approx \omega_s/2\pi$ =10 GHz) with samples that contain from roughly $N_s = 10^6$ spins to $N_s = 10^{17}$ spins, the magnetic resonance system can be configured such that $\Omega_R/2\pi$ =100 MHz, Q = 10^4 ($\kappa/2\pi$ = 1 MHz) and $g/2\pi$ = 1 Hz. For these parameters, the range of validity of the Markovian master equation is $N_s \ll \kappa^2/g^2 = 10^{12}$ and the Dicke subspace of an ensemble containing roughly 10^{11} electron spins may be polarized with an effective T_1 of 3.18 μs. This polarization time is significantly shorter than the thermal T_1 for low-temperature spin ensembles, which can range from seconds to hours.

[0098] FIG. 5 is an energy level diagram 500 of an example spin system coupled to a two-level cavity. Coherent transitions are denoted by a solid line and cavity dissipation rates are

denoted by a curved line. States in each subspace V_J are labeled $|n\rangle_c|-J_x+m\rangle_s$, where m is the number of spin excitations and n is the number of cavity excitations. Within each subspace V_J, for cooling dynamics to appear Markovian, states of high cavity excitation number should not be significantly populated on a coarse-grained timescale.

[0099] In the examples shown here, the spin ensemble is cooled by a coherent interaction with the cavity, which increases the polarization of the spin ensemble. These cavity-based cooling techniques are different from thermal T_1 relaxation, for example, because the cavity-based techniques include coherent processes over the entire spin ensemble. Thermal T_1 relaxation is an incoherent process that involves exchanging energy between individual spins and the environment, which is weakly coupled when T_1 is long. Cavity-based cooling techniques can provide a controlled enhancement of the spins' coupling to the thermal environment, by using the cavity as a link between the spin ensemble and the environment. The cavity is more strongly coupled to the environment than the spin ensemble, so energy in the form of photons is dissipated more quickly. Due to the inherently small coupling of an individual spin to the cavity, the cavity can be efficiently coupled to the spin ensemble by driving the spin ensemble so that it interacts collectively with the cavity as a single dipole moment with a greatly enhanced coupling to the cavity. In some cases, the resulting link between the spin ensemble and environment – going through the cavity – is significantly stronger than the link between the spin ensemble and the environment in the absence of the cavity, resulting in higher efficiency of energy dissipation from the spin ensemble when using the cooling algorithm, and a shorter effective T_1.

[0100] The discussion above shows how the Dicke subspace and the other subspaces are polarized by cavity-based cooling techniques. We now describe how the entire state can be cooled. Due to a global $SU(2)$ symmetry, the state space of the spin ensemble factorizes into coupled angular momentum subspaces for the spins. The largest dimension subspace is called the Dicke subspace (which corresponds to an angular momentum $J = N/2$, where N is the number of spins). For example:

$$2 \text{ spins: } (\text{Spin} - \tfrac{1}{2})^{\otimes 2} \rightarrow \text{Spin} - 1 \text{ (triplet)} \oplus \text{Spin} - 0 \text{ (singlet)}$$

$$3 \text{ spins: } (\text{Spin} - \tfrac{1}{2})^{\otimes 3} \rightarrow \text{Spin} - \tfrac{3}{2} \oplus \text{Spin} - \tfrac{1}{2} \oplus \text{Spin} - \tfrac{1}{2}.$$

As shown in FIG. 6, in the 3-spins case, the spin-3/2 subspace has the largest dimension and thus is the Dicke subspace.

[0101] FIG. 6 is a diagram 600 of an example state space represented as a 3-spin Hilbert space. The diagram 600 is a matrix representation of the 3-spin Hilbert space. The matrix has a block-diagonal form, where each block along the diagonal represents a distinct subspace. The first block represents a spin-3/2 subspace 602, and the second and third blocks represent two spin-1/2 subspaces 604a, 604b. In FIG. 6, the spin-3/2 subspace 602 is the Dicke subspace because it is the subspace of largest dimension. Cavity-based cooling can cool each respective subspace to its respective ground state. An interaction that breaks the $SU(2)$ symmetry of the Hilbert space can couple the distinct subspaces, and cavity-based cooling can cool the spin system to the true ground state of the entire Hilbert space. In the example 3-spins case shown in FIG. 6, the true ground state resides in the spin-3/2 subspace 602.

[0102] Cavity-based cooling can act independently on each subspace, cooling each subspace to its respective ground state with an effective relaxation time of

$$T_{1,J} = \frac{1}{\Gamma_S J},$$

where J is the spin of the subspace, and Γ_S is the cavity-cooling rate derived from the Markovian master equation. In some examples, the true ground state of the spin ensemble is the state where all spins are either aligned or anti-aligned with the B_0 field, and that state is in the Dicke subspace. Generally, at thermal equilibrium the spin ensemble will be in a mixed state, and there will be a distribution of states populated in all or substantially all subspaces.

[0103] The true ground state (or in some cases, another state) of the spin ensemble can be reached by coupling between the spin-J subspaces. This may be achieved by an interaction that breaks the global $SU(2)$ symmetry of the system Hamiltonian, for example, as described with respect to FIG. 1C. In some examples, the secular dipole-dipole interaction between spins, T2 relaxation, an external gradient field, or a similar external or internal dephasing interaction is sufficient to break this symmetry.

[0104] In some implementations, applying the cooling algorithm in the presence of a perturbation that breaks this symmetry allows cooling to the true ground state. In the case of the dipole-dipole interaction, simulations suggest that the spins can be cooled to the true ground state at a factor of approximately $\sqrt{N_S}/2$ times the cooling rate of the Dicke subspace. This gives an effective relaxation time to the true ground state of

$$T_{1,\,\text{dipole}} = \frac{1}{\Gamma_s\sqrt{N_s}}.$$

As in the other examples above, we consider a model that includes an exponential rate $(1/T_{1,\,\text{dipole}})$ that is analogous to the thermal spin-lattice relaxation rate $(1/T_1)$.

[0105] FIG. 7 is a plot 700 showing effective cooling times calculated for example spin ensembles. The plot 700 includes a log-scaled vertical axis 702 showing a range of cooling times in units of seconds, and a log-scaled horizontal axis 704 showing a range of values for the number of spins in the spin ensemble N_s. Three curves are shown in the plot 700. The curve 708 represents the cooling times for example spin ensembles under the thermal T_1 relaxation process. The other two curves represent the cooling times for the same example spin ensembles under the non-thermal, coherent, cavity-based cooling processes described above. In particular, the curve 706a represents the effective cooling times for a spin ensemble to reach the true ground state, and the curve 706b represents the effective cooling times for the Dicke subspace to reach its ground state.

[0106] FIG. 7 was generated based on a model of an electron spin ensemble in an X-band ESR system. In the model used for these calculations, the resonator and spin ensemble are both cooled to liquid helium temperatures (4.2 K). A typical thermal T_1 at this temperature is three seconds for a sample of irradiated quartz. The thermal T_1 is independent of the number of spins in the sample, as shown by the curve 706a in FIG. 7.

[0107] To obtain the curve 706b in FIG. 7, showing the effective cooling time constant for the Dicke subspace of a sample subjected to cavity-based cooling, we solved a Markovian master equation for a spin system having a spin-resonance frequency of 10 GHz. The model used for the calculations included a cavity-spin coupling of 1 Hz, a cavity dissipation rate of 1 MHz, a cavity detuning outside the bandwidth of the resonator, and a Rabi drive strength equal to this detuning. To obtain the curve 706a in FIG. 7, showing the effective cooling time constant for the full spin ensemble under cavity-based cooling with dipolar interaction, we based our results on small numbers of spins and extrapolated to larger numbers. Our initial findings suggest that

$$T_{1,\,\text{eff}} \approx \sqrt{N_s}T_{1,\,\text{Dicke}}.$$

As noted above, we consider a spin polarization model that evolves according to an exponential rate $(1/T_{1,\,\mathrm{eff}})$, which is analogous to the thermal spin-lattice relaxation process, which evolves according to an exponential rate $(1/T_1)$.

[0108] For the examples shown in FIG. 7, if the sample is initially restricted to the Dicke subspace, cavity-based cooling gives a speed up over thermal T_1 for samples of greater than 10^5 spins. If we consider a completely mixed sample, by including a dipolar interaction while performing cavity-based cooling of the spin ensemble, we obtain a speed up over thermal T_1 for samples of greater than 10^{10} spins.

[0109] In the model for cavity-based cooling of a spin ensemble presented above, several assumptions are made for illustration purposes. In some instances, the results and advantages described above can be achieved in systems that do not adhere to one or more of these assumptions. First, we have assumed that the spin ensemble is magnetically dilute such that no coupling exists between spins. A spin-spin interaction that breaks the global $SU(2)$ symmetry of the Tavis-Cummings (TC) Hamiltonian will connect the spin-J subspaces in the coupled angular momentum decomposition of the state space. Such an interaction may be used as an additional resource that should permit complete polarization of the full ensemble Hilbert space. Second, we have neglected the effects of thermal relaxation of the spin system. In some instances, as the cooling effect of the cavity on the spin system relies on a coherent spin-cavity information exchange, the relaxation time of the spin system in the frame of the Rabi drive – commonly referred to as $T_{1,\rho}$ – should be significantly longer than the inverse cavity dissipation rate $1/\kappa$. Third, we have assumed that the spin-cavity coupling and Rabi drive are spatially homogeneous across the spin ensemble. Inhomogeneities may be compensated for, for example, by numerically optimizing a control pulse that implements an effective spin-locking Rabi drive of constant strength over a range of spin-cavity coupling and control field amplitudes.

[0110] In some implementations, the ability of the cavity to remove energy from the spin system depends at least partially on the cooling power of the cooling system used to cool the cavity. In the example simulations presented above, the cooling power of the cooling system is taken to be infinite, corresponding to an infinite heat capacity of the cavity. The techniques described here can be implemented in a system where the cavity has a finite heat capacity. In FIGS. 8A and 8B, we give a model of the flow of entropy and energy in an example cavity-based cooling process.

[0111] FIG. 8A is a schematic diagram 800 showing entropy flow in an example cavity-based cooling process. In the diagram 800, the spins 802 represent a spin ensemble, the cavity 804 represents a cavity that is coupled to the spin ensemble, for example, under the conditions described above, and the fridge 806 represents a refrigerator or another type of cooling system that cools the cavity. Energy removed from the spin ensemble flows to the cavity at a rate of Γ_{SC}, and energy is removed from the cavity at a rate of Γ_{CF} by the (finite) cooling power of the refrigerator.

[0112] FIG. 8B is a plot 810 showing example values of the dissipation rates Γ_{SC} and Γ_{CF}. The plot 810 includes a vertical axis 812 representing a range of values for cooling power in units of microwatts (μW), and a log-scaled horizontal axis 814 showing a range of values for the number of spins in the spin ensemble N_s. Because the cooling power of the fridge 806 is held constant in the simulations represented in the plot 810, the rate Γ_{CF} of entropy removal from the cavity to the refrigerator remains constant, as shown by the curve 816a. The rate Γ_{SC} of entropy removal from the spin ensemble to the cavity, represented by the curve 816b, was calculated by specifying the total energy to be removed from the spin system to polarize it divided by the time over which that energy is removed, calculated based on our derived cooling times. The total energy removed from the spin system was calculated as $(N_s/2)\hbar\omega$, where ω was taken to be $2\pi 10$ GHz. In the examples shown, the spin system is an electron spin ensemble that starts in the fully mixed state such that half the spins must be driven to their ground state.

[0113] Energy deposited into the cavity is removed by the fridge at a rate that is based on the cooling power of the fridge, which is typically on the order of tens of microwatts (as shown in FIG. 8B) in some example applications. The curve 816b in FIG. 8B demonstrates that under some conditions, for ensembles larger than roughly 10^{13} electron spins, a bottleneck of entropy flow may exist that will limit the minimum cooling time for larger ensembles. However, in the example shown, an ensemble of 10^{12} electron spins may be cooled in roughly 3.18 microseconds (μs) given a fridge with cooling power of 50 μW. An ensemble of this size is sufficient to obtain a strong electron spin resonance signal.

[0114] Finally, the derivation of the Markovian master equation above assumes that no correlations between cavity and spin system accrue during the cooling process, such that there is no back action of the cavity dynamics on the spin system. This condition is enforced when the cavity dissipation rate, κ, exceeds the rate of coherent spin-cavity exchange in the

lowest excitation manifold by at least an order of magnitude (i.e. $\kappa \geq 10g\sqrt{N_s}$). In this Markovian limit, the rate at which spin photons are added to the cavity is significantly less than the rate at which thermal photons are added, meaning the cooling power of the fridge necessary to maintain the thermal cavity temperature is sufficient to dissipate the spin photons without raising the average occupation number of the cavity. From the above equation we see that the cooling efficiency could be improved by adding more spins to make κ closer to $g\sqrt{N_s}$; in this regime the cooling power of the fridge may not be sufficient to prevent back action from the cavity and non-Markovian effects significantly lower the cooling rate.

[0115] The techniques described above can be implemented in a magnetic resonance imaging (MRI) system and in other environments. FIG. 9 is a schematic diagram of an example MRI system 900. The example MRI system 900 includes a scanner 910, a computer system 930 and a sample holder 920 for holding a sample 922. The sample holder 920 includes a temperature control system 924 that can regulate the temperature of the sample 922. The scanner includes a primary magnet system 912, a gradient system 914, a cooling system 916, and a resonator and cavity system 918. An MRI system can include additional or different features, and the features of an MRI system can be arranged as shown in FIG. 9 or in another manner.

[0116] The example primary magnet system 912 is designed to provide a substantially constant, homogeneous external magnetic field. For example, the primary magnet system 912 may operate as the primary magnet system 102 shown in FIG. 1A. The example gradient system 914 includes one or more gradient coils designed to provide magnetic field gradients (e.g., gradients along Cartesian axes). For example, the gradient system 914 may operate as the gradient system 140 shown in FIG. 1A. The gradient fields can be configured to acquire image data of a desired slice or region of the sample 922, for example, by generating a phase-encoding or slice-selecting field.

[0117] The resonator and cavity system 918 can polarize and control a spin ensemble in the sample 922. For example, the resonator and cavity system 918 may operate as the resonator and cavity system 112 shown in FIG. 1A. The resonator and cavity system 918 can include a cavity and a resonator, which can be implemented as an integrated multi-mode resonator structure or as multiple distinct structures. The resonator and cavity system 918 can include radio-frequency coils designed to transmit and receive radio-frequency pulses. For example,

to acquire an image from the sample 922, the resonator and cavity system 918 can execute an imaging pulse sequence in concert with a gradient sequence executed by the gradient system 914. In some instances, the resonator and cavity system 918 can include various types of coils that can be placed around specific parts of a body (e.g., the head, knee, wrist, etc.) or be internally implanted in an imaging subject, depending on the sample and imaging applications. In some implementations, the resonator and cavity components that are used to polarize the spin ensemble (e.g., as described with respect to FIG. 1A) may also be used to apply an imaging pulse sequence to the sample 922. In some implementations, separate radio-frequency coils are used to apply the imaging pulse sequence.

[0118] The example cooling system 916 can control the temperature of all or part of the resonator and cavity system 918. For example, the cooling system 916 may operate as the example cooling system 120 shown in FIG. 1A. In some cases, the cooling system 916 maintains the cavity, and possibly other components of the resonator and cavity system 918, below the temperature of the sample 922. For example, the cooling system 916 can provide cooling down to cryogenic temperatures in some implementations.

[0119] In some instances, the temperature control system 924 regulates the temperature of the sample 922. For example, temperature control system 924 may operate as the example temperature control system 130 shown in FIG. 1A. In some cases, the temperature control system 924 maintains the sample 922 at room temperature, or another temperature that is appropriate for an imaging subject. For example, the imaging subject can be held at liquid-state temperatures, or a live imaging subject (e.g., a human) can be held at an appropriate temperature.

[0120] In some aspects of operation, the resonator and cavity system 918 interacts with a spin ensemble (e.g., Hydrogen spins) in the sample 922 to prepare the spin ensemble for an imaging scan. In some implementations, the resonator and cavity system 918 executes a cavity-based cooling process that brings the spin ensemble to a higher level of polarization than the spin ensemble's thermal equilibrium state (i.e., greater than the polarization produced by thermal relaxation in the particular temperature and magnetic field environment). In some implementations, the cavity-based cooling process increases the spin ensemble's polarization at a rate that is faster than the thermal T_1 relaxation rate. The resulting polarized state of the spin ensemble can be used as an initial state for an imaging scan. After each imaging scan, the spin ensemble can be re-polarized for further scans. In some cases, the cavity-based cooling process reduces the duration of the imaging process, for

example, by reducing the number of imaging scans required. In some cases, the cavity-based cooling process improves the quality of the image produced, for example, by increasing the signal-to-noise ratio of an imaging scan.

[0121] While this specification contains many details, these should not be construed as limitations on the scope of what may be claimed, but rather as descriptions of features specific to particular examples. Certain features that are described in this specification in the context of separate implementations can also be combined. Conversely, various features that are described in the context of a single implementation can also be implemented in multiple embodiments separately or in any suitable subcombination.

[0122] Example implementations of several independent, general concepts have been described. In one general aspect of what is described above, a drive field is applied to a spin ensemble in a static magnetic field. The drive field is adapted to couple spin states of the spin ensemble with one or more cavity modes of a cavity. Polarization of the spin ensemble is increased by the coupling between the spin states and the cavity mode.

[0123] In another general aspect of what is described above, a cavity is coupled with a spin ensemble in a sample. The sample can be held at a thermal temperature and subject to a static magnetic field, and an interaction between the cavity and the spin ensemble is generated (e.g., by applying a drive field). The interaction increases polarization of the spin ensemble faster than the internal polarizing process affecting the sample.

[0124] In another general aspect of what is described above, a thermal barrier thermally insulates between a sample and a cavity. The cavity is at a first temperature, and the sample is at a second, different temperature. The sample contains a spin ensemble in a static magnetic field. An interaction between the cavity and the spin ensemble is generated. The interaction increases polarization of the spin ensemble.

[0125] In another general aspect of what is described above, a magnetic resonance imaging (MRI) system includes a cavity adapted to interact with a spin ensemble in a sample in a static magnetic field. The sample is an imaging subject. The MRI system includes a resonator adapted to generate an interaction between the cavity and the spin ensemble that increases polarization of the spin ensemble. The MRI system can acquire a magnetic resonance signal from the polarized spin ensemble in the imaging subject, and an image of the imaging subject can be generated based on the magnetic resonance signal. In some cases, the imaging subject

is held at room temperature, for example, at 296 Kelvin, 300 Kelvin, or another appropriate temperature between 290 and 310 Kelvin.

[0126] In some implementations of the general concepts described above, the temperature of the cavity is regulated by a cooling system that is thermally coupled to the cavity, and the temperature of the sample is regulated by a sample temperature control system. The cavity can be maintained at a cryogenic temperature, and the sample can be maintained in a liquid state. The cavity can be maintained below 100 Kelvin, and the sample can be maintained above 273 Kelvin (e.g., at room temperature or another temperature). In some cases, the thermal barrier inhibits thermal interaction between the sample and the cavity.

[0127] In some implementations of the general concepts described above, polarization of the spin ensemble is increased by cavity-based cooling acting independently on each angular momentum subspace of the spin ensemble via the coupling between the spin states and the cavity mode, and a mixing process mixing the angular momentum subspaces. The operations can be applied iteratively in some instances. The angular momentum subspaces can be mixed, for example, by a dipolar interaction, a transverse (T_2) relaxation process, application of a gradient field, or a combination of these and other processes.

[0128] In some implementations of the general concepts described above, the cavity has a low mode volume and a high quality factor. The mode volume, the quality factor, or a combination of these and other cavity parameters can be designed to produce a coupling between the spin ensemble and the cavity that effectively "short-circuits" the spin ensemble polarization process. In some examples, the cavity has a mode volume V and a quality factor Q, such that $\kappa \gg g\sqrt{N_s}$. Here, N_s represents the number of spins in the spin ensemble, $\kappa = (\omega_c/Q)$ represents the dissipation rate of the cavity, ω_c represents the resonance frequency of the cavity, and g represents the coupling strength of the cavity to an individual spin in the spin ensemble. In some examples, the dissipation rate κ is more than two times $g\sqrt{N_s}$. In some examples, the dissipation rate κ is an order of magnitude greater than $g\sqrt{N_s}$. In some examples, the dissipation rate κ is two or three orders of magnitude greater than $g\sqrt{N_s}$. In some instances, the coupling between the spin ensemble and the cavity increases polarization of the spin ensemble faster than the thermal spin-lattice (T_1) relaxation process.

[0129] In some implementations of the general concepts described above, the spin ensemble has a spin-resonance frequency (ω_s), and the drive field is generated by a resonator that is on-resonance with the spin-resonance frequency (ω_s). The drive field can be a time-varying

(e.g., oscillating or otherwise time-varying) magnetic field. In some cases, the spin ensemble is a nuclear spin ensemble, and the drive field is a radio-frequency field. In some cases, the spin ensemble is an electron spin ensemble, and the drive field is a microwave-frequency field.

[0130] In some implementations of the general concepts described above, the cavity mode corresponds to a cavity-resonance frequency (ω_c), and the cavity-resonance frequency (ω_c) is detuned from the spin-resonance frequency (ω_s) by an amount $\delta\omega = \omega_s - \omega_c$. The drive field can have a drive field strength that generates Rabi oscillations at a Rabi frequency (Ω_R). In some cases, the detuning $\delta\omega$ is substantially equal to Ω_R. For instance, the difference $\Delta = \delta\omega - \Omega_R$ can be small compared to the detuning $\delta\omega$. In some examples, the difference Δ is less than half the detuning $\delta\omega$. In some examples, the difference Δ is an order of magnitude less than the detuning $\delta\omega$. In some examples, the difference Δ is two or three orders of magnitude less than the detuning $\delta\omega$.

[0131] In some implementations of the general concepts described above, the interaction between the cavity and the spin ensemble increases polarization of the spin ensemble at a polarization rate that is related to a parameter of the cavity. In some instances, the polarization rate can be higher or lower due to an electromagnetic property of the cavity, such as the value of the quality factor, the value of the mode volume, the value of the dissipation rate, or another property.

[0132] In some implementations of the general concepts described above, the static magnetic field is applied to the spin ensemble by a primary magnet system, and the static magnetic field is substantially uniform over the spin ensemble. The drive field can be oriented orthogonal to the static magnetic field. For example, the static magnetic field can be oriented along a z-axis, and the drive field can be oriented in the xy-plane (which is orthogonal to the z-axis).

[0133] In some implementations of the general concepts described above, the drive field is generated by a resonator. In some cases, the resonator and cavity are formed as a common structure or subsystem. For example, the resonator and cavity can be integrated in a common, multi-mode resonator structure. In some cases, the resonator and cavity are formed as two or more separate structures. For example, the resonator can be a coil structure having a first resonance frequency, and the cavity can be a distinct cavity structure that has a second,

different resonance frequency. The resonator, the cavity, or both can include superconducting material and other materials.

[0134] In some implementations of the general concepts described above, the coupling between the spin ensemble and the cavity changes the state of the spin ensemble. For example, the coupling can map the spin ensemble from an initial (mixed) state to a subsequent state that has higher polarization than the initial state. The subsequent state can be a mixed state or a pure state. In some cases, the subsequent state has a purity that is equal to the purity of the cavity. In some instances, the coupling can evolve the spin ensemble from an initial state to the thermal equilibrium state of the spin ensemble, or to another state that has higher polarization than the thermal equilibrium state. The thermal equilibrium state is typically defined, at least partially, by the sample environment (including the sample temperature and the static magnetic field strength). In some instances, the coupling can evolve the spin ensemble from an initial state to a subsequent state having a polarization that is less than, equal to, or greater than the thermal equilibrium polarization.

[0135] In some implementations of the general concepts described above, the drive field is adapted to couple the Dicke subspace of the spin ensemble with the cavity modes. In some representations of the spin ensemble, the Dicke subspace can be defined as the largest angular momentum subspace, such that the Dicke subspace contains all the totally-symmetric states of the spin ensemble. In some representations, the Dicke subspace corresponds to a system with total angular momentum $J = N_S/2$, where N_S is the number of spins in the spin ensemble. In some cases, the Dicke subspace and multiple other angular momentum subspaces of the spin ensemble are coupled with the cavity modes. In some cases, all angular momentum subspaces of the spin ensemble are coupled with the cavity modes.

[0136] In some implementations of the general concepts described above, the interaction between the cavity and the spin ensemble causes the spin ensemble to dissipate photons to a thermal environment via the cavity modes. The interaction can include a coherent radiative interaction between the cavity and the spin ensemble. In some cases, the coherent radiative interaction can increase the spin ensemble's polarization faster than any incoherent thermal process (e.g., thermal spin-lattice relaxation, spontaneous emission, etc.) affecting the spin ensemble. In some cases, the interaction drives the spin ensemble so that it interacts collectively with the cavity as a single dipole moment.

[0137] A number of embodiments have been described. Nevertheless, it will be understood that various modifications can be made. Accordingly, other embodiments are within the scope of the following claims.

CLAIMS

1. A magnetic resonance imaging (MRI) system comprising:

a cavity adapted to interact with a spin ensemble in an imaging subject in a static magnetic field;

a resonator adapted to generate an interaction between the cavity and the spin ensemble that increases polarization of the spin ensemble; and

a control system operable to acquire a magnetic resonance signal from the imaging subject.

2. The MRI system of claim 1, further comprising a computer system operable to generate an image of the imaging subject based on the magnetic resonance signal.

3. The MRI system of claim 1, further comprising a sample holder that supports the imaging subject in the static magnetic field.

4. The MRI system of claim 1, further comprising a thermal barrier that thermally insulates the cavity from the imaging subject.

5. The MRI system of claim 1, wherein the interaction brings the spin ensemble to a higher polarization than the spin ensemble's thermal equilibrium polarization in the static magnetic field.

6. The MRI system of claim 1, further comprising:

a cooling system adapted to regulate a temperature of the cavity; and

a temperature control system adapted to regulate a temperature of the imaging subject.

7. The MRI system of claim 6, wherein the cooling system is adapted to maintain the cavity at a temperature that is below 100 Kelvin, and the temperature control system is adapted to maintain the imaging subject at a temperature that is above 273 Kelvin.

8. The MRI system of claim 6, wherein the temperature control system includes a thermal barrier adapted to thermally insulate between the imaging subject and the cavity.

9. The MRI system of claim 6, wherein the cooling system includes a thermal barrier adapted to thermally insulate between the imaging subject and the cavity.

10. The MRI system of claim 1, wherein the resonator and the cavity are distinct structures.

11. The MRI system of claim 1, comprising an integrated multi-mode resonator structure that includes the resonator and the cavity.

12. A magnetic resonance imaging (MRI) method comprising:

thermally insulating between an imaging subject and a cavity, the cavity being at a first temperature, the imaging subject being at a second, different temperature and containing a spin ensemble in a static magnetic field;

generating an interaction between the cavity and the spin ensemble that increases polarization of the spin ensemble; and

acquiring a magnetic resonance signal from the imaging subject.

13. The MRI method of claim 12, comprising:

regulating a temperature of the cavity by operation of a cooling system that is thermally coupled to the cavity; and

regulating a temperature of the imaging subject by a temperature control system.

14. The MRI method of claim 13, wherein regulating a temperature of the cavity comprises maintaining the cavity at a cryogenic temperature, and regulating a temperature of the imaging subject comprises maintaining the imaging subject in a liquid state.

15. The MRI method of claim 13, wherein regulating a temperature of the cavity comprises maintaining the cavity at a temperature that is below 100 Kelvin, and regulating a temperature of the imaging subject comprises maintaining the imaging subject at a room temperature between 290 and 310 Kelvin.

16. The MRI method of claim 12, wherein thermally insulating comprises a solid thermal barrier inhibiting thermal interaction between the imaging subject and the cavity.

17. The MRI method of claim 12, comprising increasing polarization of the spin ensemble by iteratively:

acting on angular momentum subspaces of the spin ensemble by the interaction between the spin ensemble and the cavity; and

mixing the angular momentum subspaces.

18. The MRI method of claim 17, where the angular momentum subspaces are mixed by at least one of a dipolar interaction, a transverse (T_2) relaxation process, or application of a gradient field.

19. The MRI method of any of claims 12-18, wherein the interaction brings the spin ensemble to a higher polarization than the spin ensemble's thermal equilibrium polarization at the second temperature in the static magnetic field.

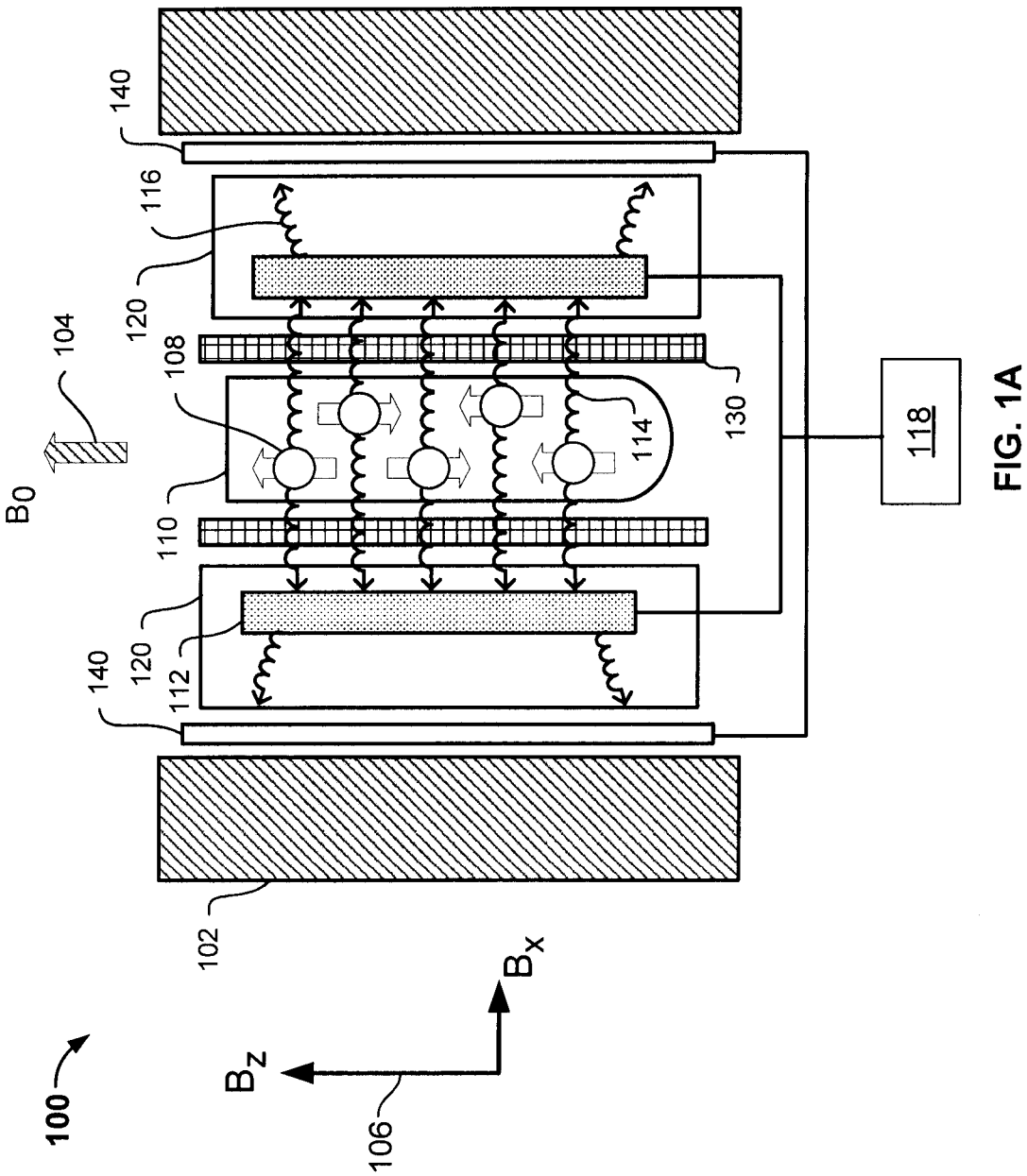

140
116
120
104
108
B0
110
114
130
118
120
112
140
102
100
Bz
Bx
106

FIG. 1A

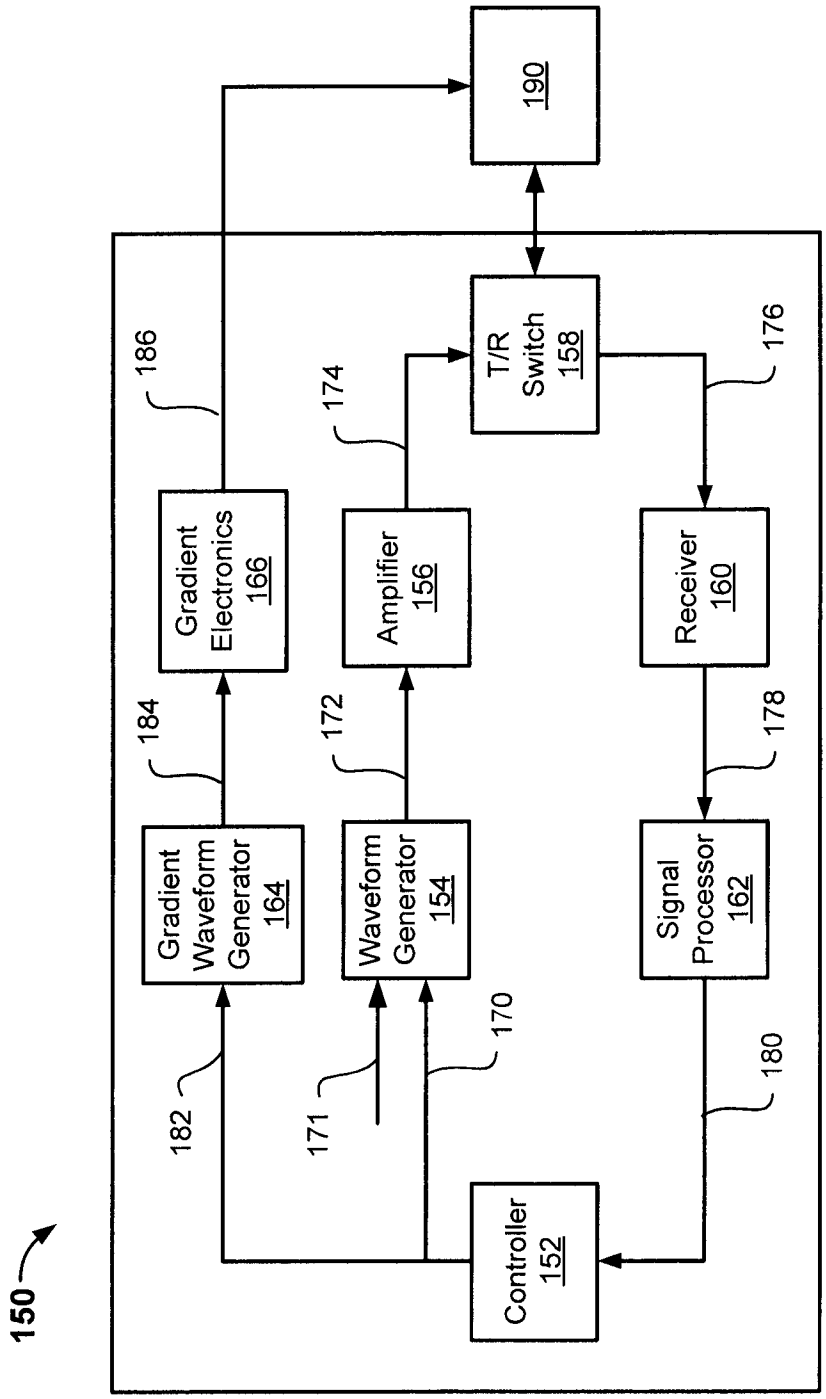

150
190
T/R Switch 158
Gradient Electronics 166
Amplifier 156
Receiver 160
Gradient Waveform Generator 164
Waveform Generator 154
Signal Processor 162
Controller 152
186
174
176
184
172
178
182
171
170
180

FIG. 1B

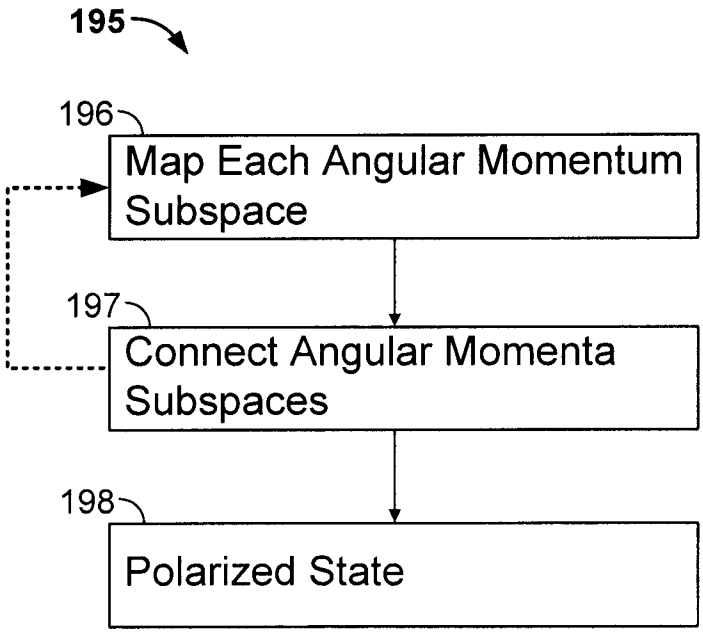

195
196
Map Each Angular Momentum Subspace
197
Connect Angular Momenta Subspaces
198
Polarized State

FIG. 1C

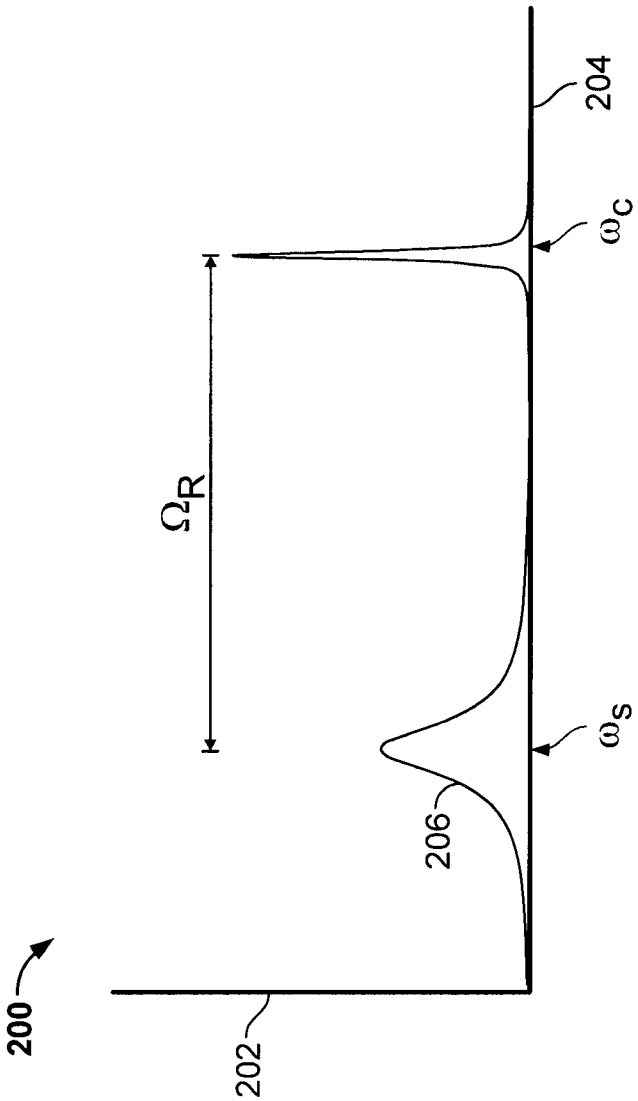


FIG. 2

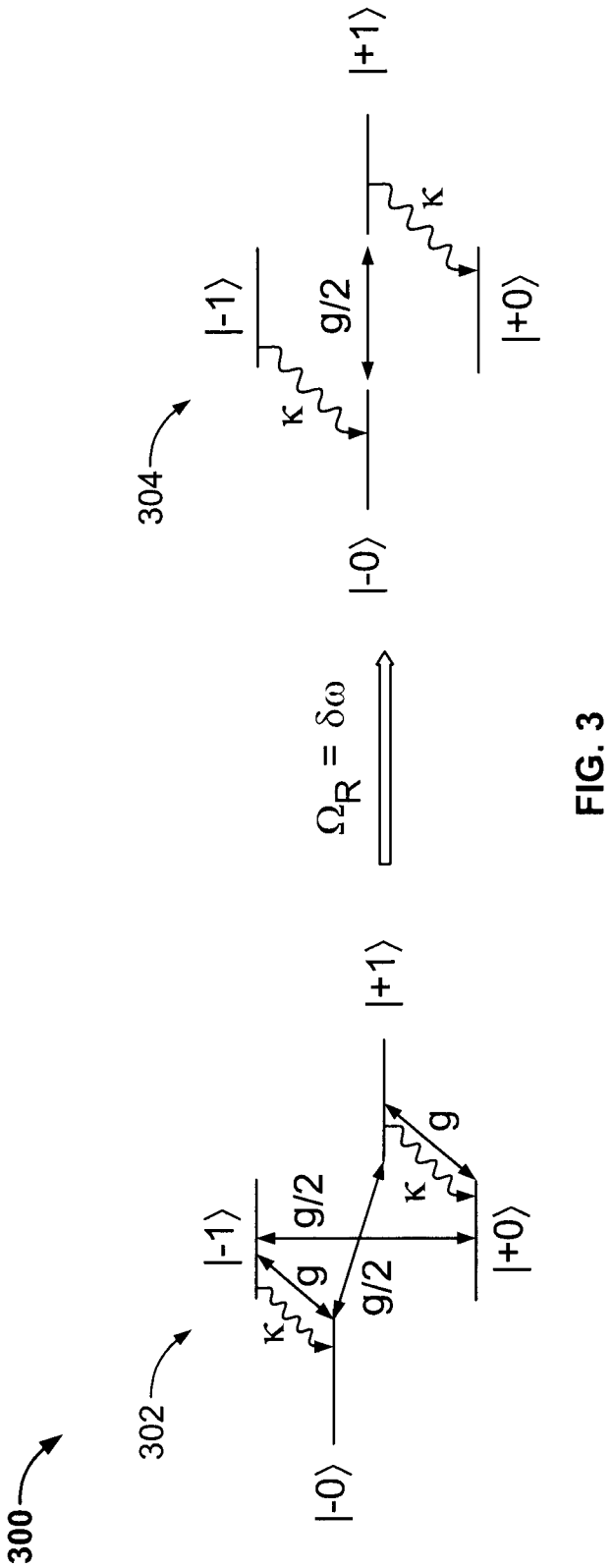


FIG. 3

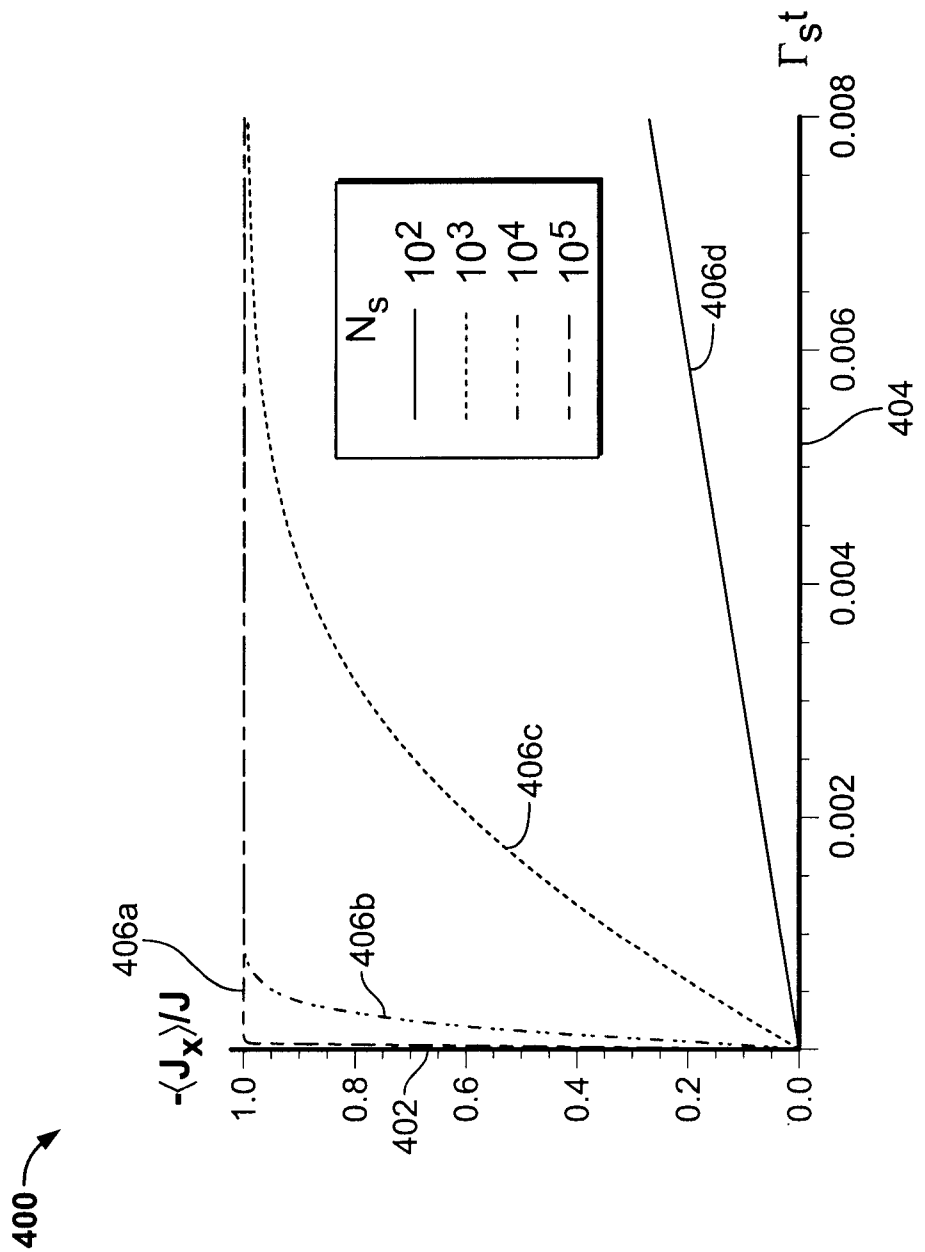

400
$-\langle J_x \rangle / J$
1.0
0.8
402
0.6
0.4
0.2
0.0
406a
406b
406c
406d
N_s
10^2
10^3
10^4
10^5
0.002
0.004
404
0.006
0.008
$\Gamma_s t$

FIG. 4

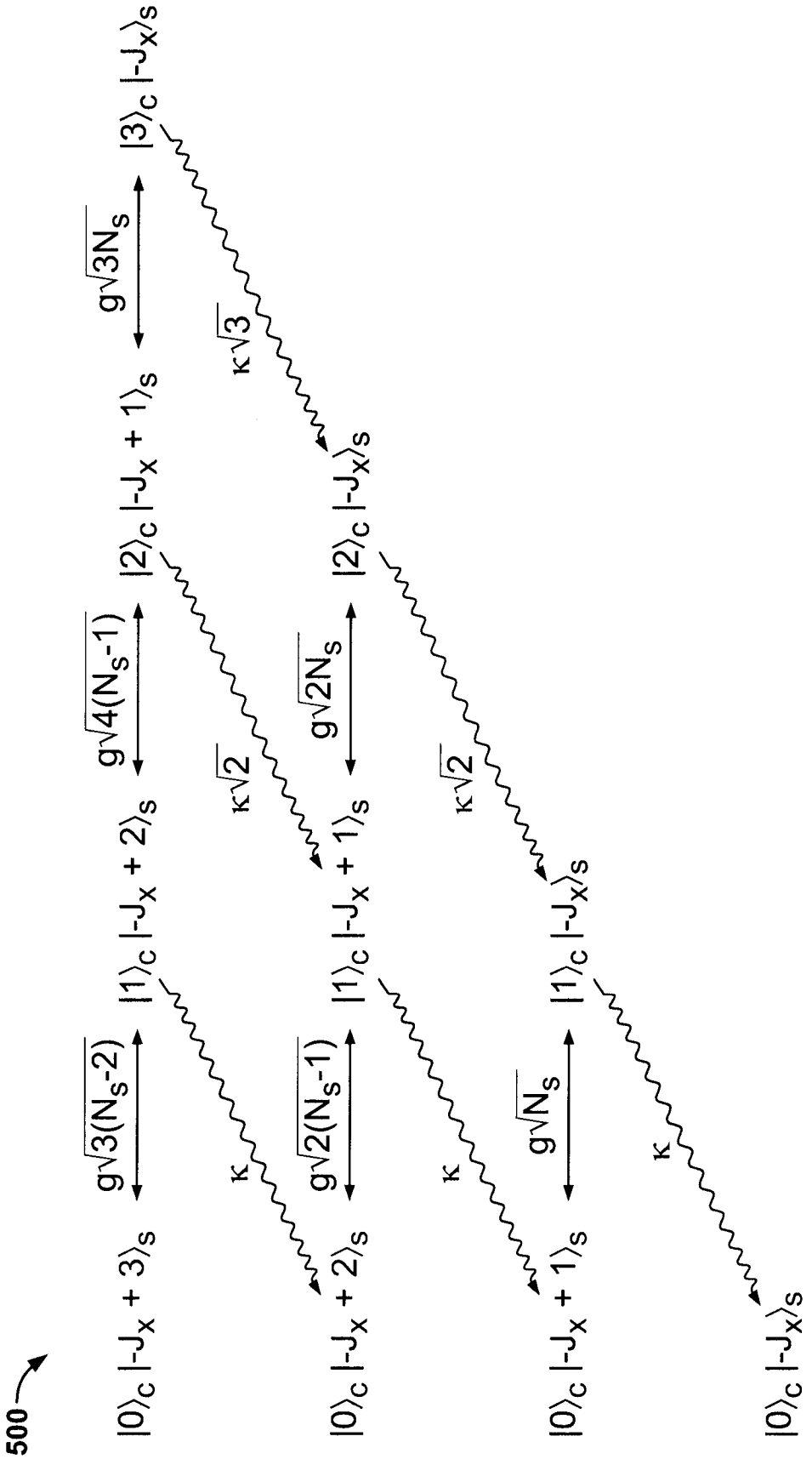

500
$|0\rangle_C |-J_X + 3\rangle_S$
$g\sqrt{3(N_S-2)}$
$|1\rangle_C |-J_X + 2\rangle_S$
$g\sqrt{4(N_S-1)}$
$|2\rangle_C |-J_X + 1\rangle_S$
$g\sqrt{3N_S}$
$|3\rangle_C |-J_X\rangle_S$
κ
$\kappa\sqrt{2}$
$\kappa\sqrt{3}$
$|0\rangle_C |-J_X + 2\rangle_S$
$g\sqrt{2(N_S-1)}$
$|1\rangle_C |-J_X + 1\rangle_S$
$g\sqrt{2N_S}$
$|2\rangle_C |-J_X\rangle_S$
κ
$\kappa\sqrt{2}$
$|0\rangle_C |-J_X + 1\rangle_S$
$g\sqrt{N_S}$
$|1\rangle_C |-J_X\rangle_S$
κ
$|0\rangle_C |-J_X\rangle_S$

FIG. 5

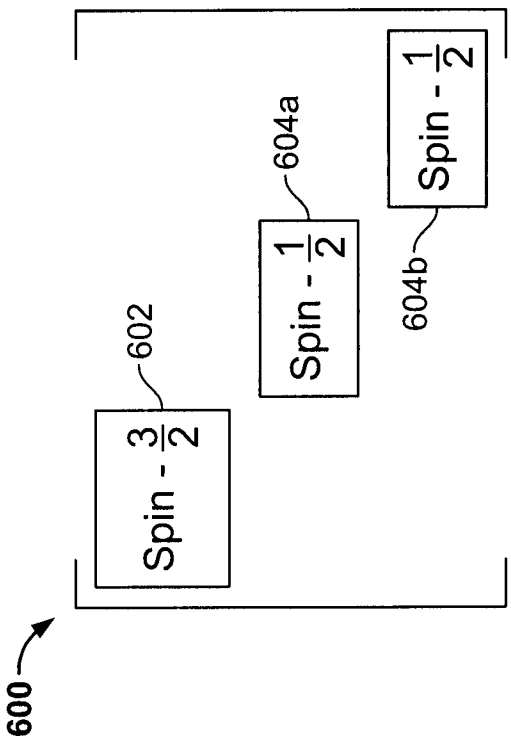

600
602
Spin - 3/2
604a
Spin - 1/2
604b
Spin - 1/2

FIG. 6

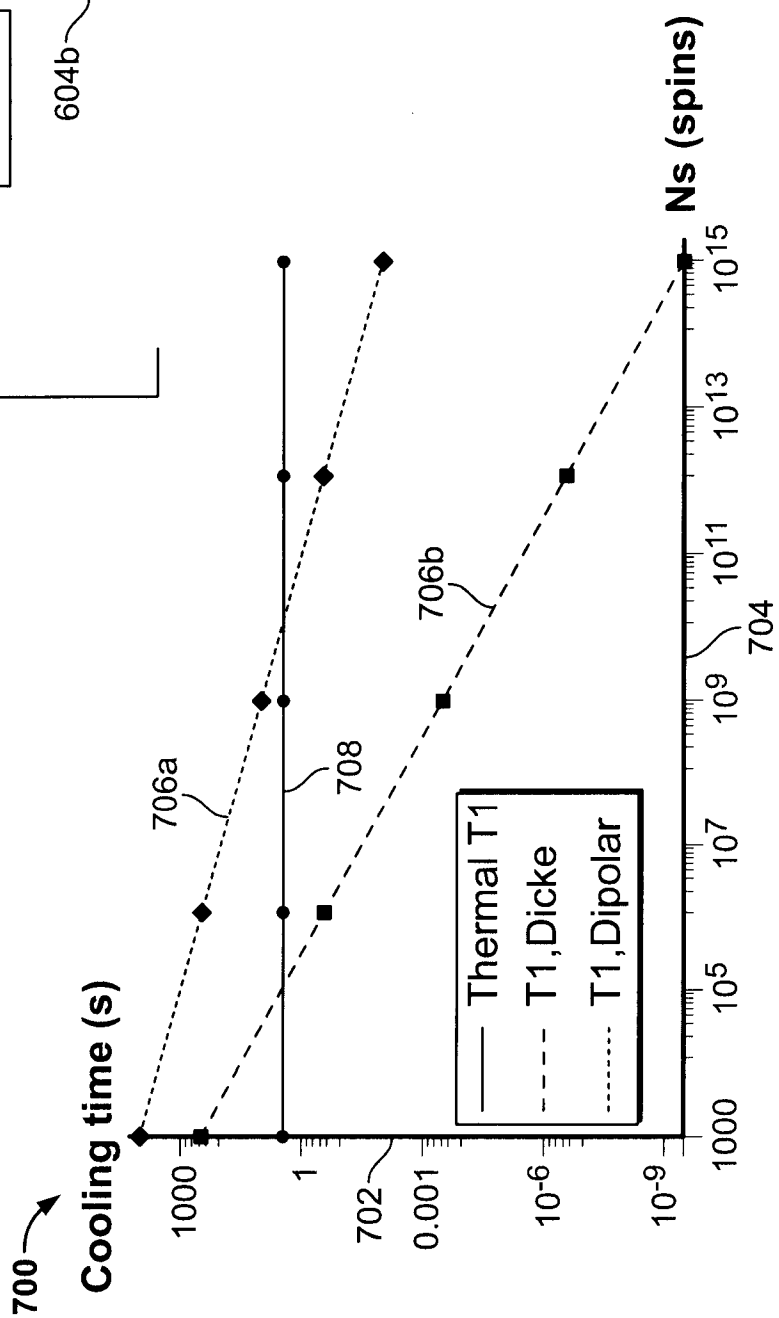

700
Cooling time (s)
1000
1
0.001
10^{-6}
10^{-9}
702
706a
708
706b
704
Ns (spins)
1000
10^5
10^7
10^9
10^{11}
10^{13}
10^{15}
Thermal T1
T1,Dicke
T1,Dipolar

FIG. 7

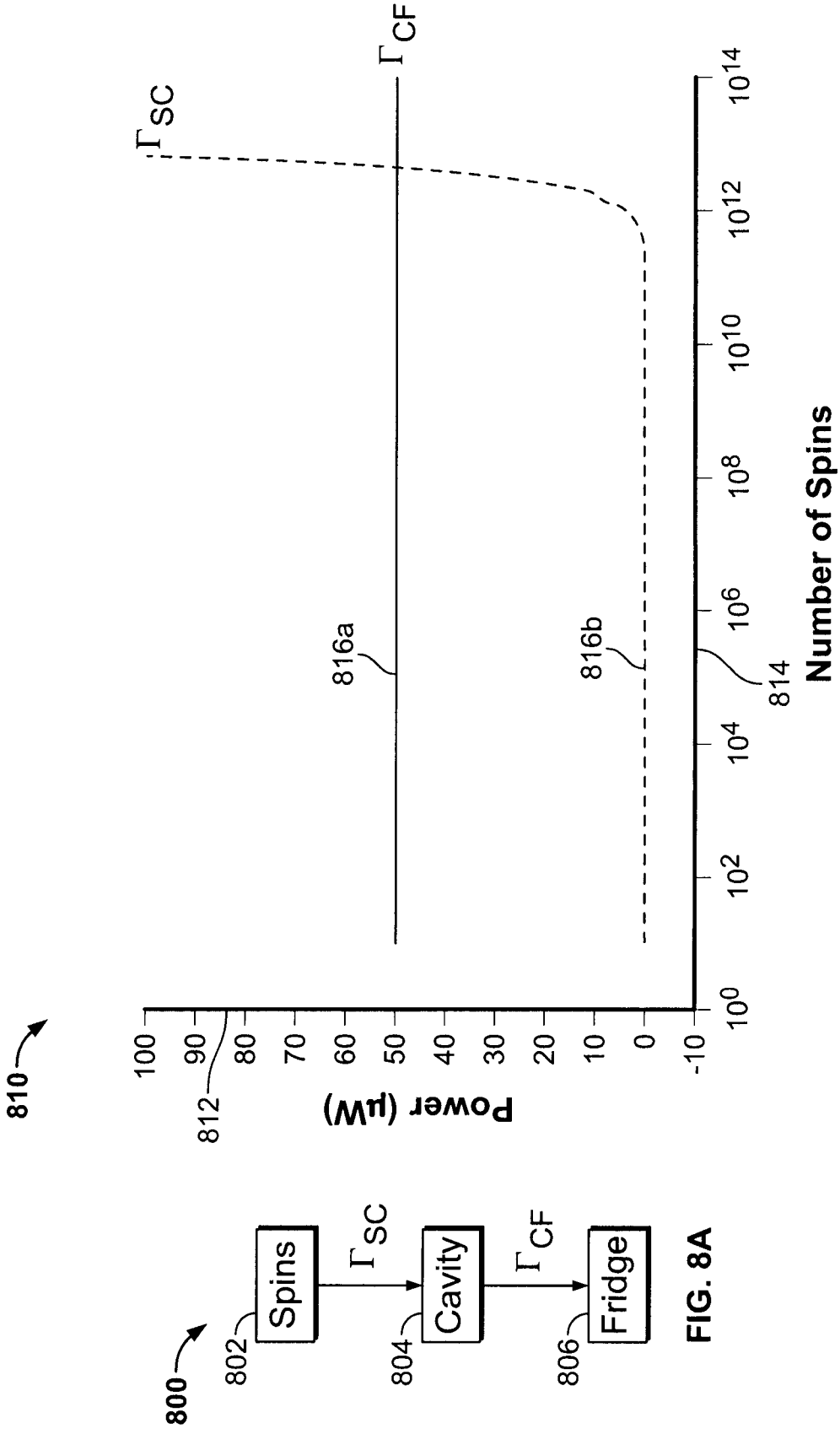

800
802
Spins
Γ_{SC}
804
Cavity
Γ_{CF}
806
Fridge
810
812
Power (μW)
100
90
80
70
60
50
40
30
20
10
0
-10
Γ_{SC}
Γ_{CF}
816a
816b
814
10^0
10^2
10^4
10^6
10^8
10^{10}
10^{12}
10^{14}
Number of Spins

FIG. 8A

FIG. 8B

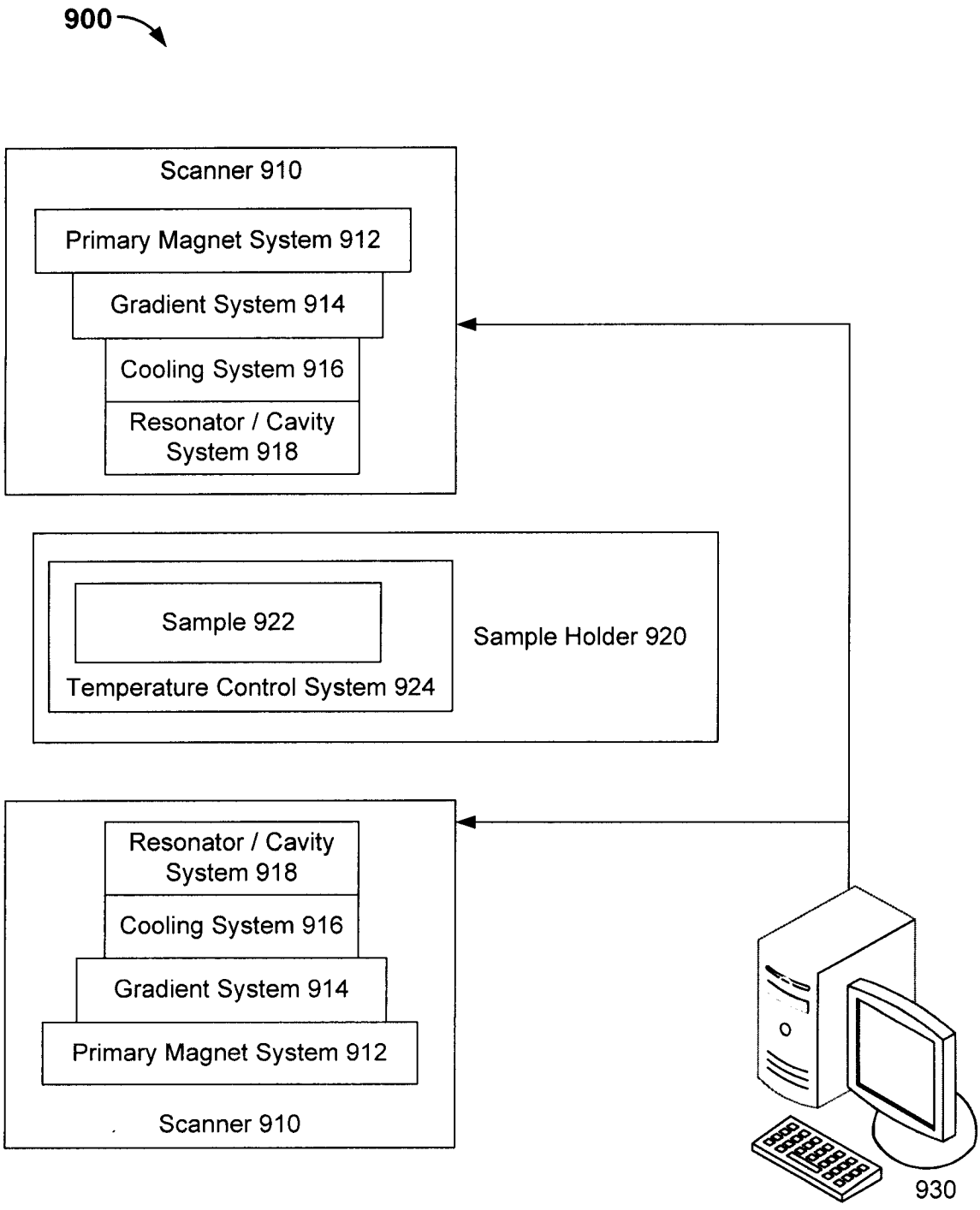

900
Scanner 910
Primary Magnet System 912
Gradient System 914
Cooling System 916
Resonator / Cavity System 918
Sample 922
Temperature Control System 924
Sample Holder 920
Resonator / Cavity System 918
Cooling System 916
Gradient System 914
Primary Magnet System 912
Scanner 910
930

FIG. 9

INTERNATIONAL SEARCH REPORT

International application No.
PCT/CA2014/000066

A. CLASSIFICATION OF SUBJECT MATTER
IPC: ***G01R 33/31*** (2006.01), ***A61B 5/055*** (2006.01), ***G01R 33/30*** (2006.01)

According to International Patent Classification (IPC) or to both national classification and IPC

B. FIELDS SEARCHED

Minimum documentation searched (classification system followed by classification symbols)
IPC: ***G01R 33/31*** (2006.01), ***A61B 5/055*** (2006.01), ***G01R 33/30*** (2006.01)

Documentation searched other than minimum documentation to the extent that such documents are included in the fields searched

Electronic database(s) consulted during the international search (name of database(s) and, where practicable, search terms used)
Google, Canadian patents database, espacenet, Epodoc

C. DOCUMENTS CONSIDERED TO BE RELEVANT

Category*	Citation of document, with indication, where appropriate, of the relevant passages	Relevant to claim No.
X	US 2001/013779 A1 (Marek, D.) 16 August 2001 (16-08-2001)	1-19
X Y	Purdy, T.P. et al., "Cavity-aided magnetic resonance microscopy of atomic transport in optical lattices", Nature Physics (Impact Factor: 19.35). 01/2011; 7(8):604-607. DOI: 10.1038/nphys1967, URL http://ultracold.physics.berkeley.edu/pmwiki/uploads/Main/CAMRI.pdf	1-11 12-19
X Y	Torrezan, A.C. et al., "Microstrip resonators for electron paramagnetic resonance experiments", Review of Scientific Instruments 80, 075111, 31 July 2009 (31-07-2009); doi: 10.1063/1.3186054	1-11 12-19
X Y	Kubo, Y. et al., "Strong Coupling of a Spin Ensemble to a Superconducting Resonator", Physical Review Letters 105, 140502, 27 September 2010 (27-09-2010), pages 1-4, DOI: 10.1103/PhysRevLett.105.140502	1-11 12-19
Y	US 6677751 B1 (Marek, D. et al.) 13 January 2004 (13-01-2004)	12-19

☐ Further documents are listed in the continuation of Box C.

☑ See patent family annex.

*	Special categories of cited documents:
"A"	document defining the general state of the art which is not considered to be of particular relevance
"E"	earlier application or patent but published on or after the international filing date
"L"	document which may throw doubts on priority claim(s) or which is cited to establish the publication date of another citation or other special reason (as specified)
"O"	document referring to an oral disclosure, use, exhibition or other means
"P"	document published prior to the international filing date but later than the priority date claimed
"T"	later document published after the international filing date or priority date and not in conflict with the application but cited to understand the principle or theory underlying the invention
"X"	document of particular relevance; the claimed invention cannot be considered novel or cannot be considered to involve an inventive step when the document is taken alone
"Y"	document of particular relevance; the claimed invention cannot be considered to involve an inventive step when the document is combined with one or more other such documents, such combination being obvious to a person skilled in the art
"&"	document member of the same patent family

Date of the actual completion of the international search 28 March 2014 (28-03-2014)	Date of mailing of the international search report 01 May 2014 (01-05-2014)
Name and mailing address of the ISA/CA Canadian Intellectual Property Office Place du Portage I, C114 - 1st Floor, Box PCT 50 Victoria Street Gatineau, Quebec K1A 0C9 Facsimile No.: 001-819-953-2476	Authorized officer Valérie Dubé (819) 934-4261

Box No. II **Observations where certain claims were found unsearchable (Continuation of item 2 of the first sheet)**

This international search report has not been established in respect of certain claims under Article 17(2)(a) for the following reasons:

1. ☐ Claim Nos.:
because they relate to subject matter not required to be searched by this Authority, namely:

2. ☐ Claim Nos.:
because they relate to parts of the international application that do not comply with the prescribed requirements to such an extent that no meaningful international search can be carried out, specifically:

3. ☐ Claim Nos.:
because they are dependent claims and are not drafted in accordance with the second and third sentences of Rule 6.4(a).

Box No. III **Observations where unity of invention is lacking (Continuation of item 3 of first sheet)**

This International Searching Authority found multiple inventions in this international application, as follows:

See extra sheet for details

1. ☐ As all required additional search fees were timely paid by the applicant, this international search report covers all searchable claims.

2. ☑ As all searchable claims could be searched without effort justifying additional fees, this Authority did not invite payment of additional fees.

3. ☐ As only some of the required additional search fees were timely paid by the applicant, this international search report covers only those claims for which fees were paid, specifically claim Nos.:

4. ☐ No required additional search fees were timely paid by the applicant. Consequently, this international search report is restricted to the invention first mentioned in the claims; it is covered by claim Nos.:

Remark on Protest

☐ The additional search fees were accompanied by the applicant's protest and, where applicable, the payment of a protest fee.

☐ The additional search fees were accompanied by the applicant's protest but the applicable protest fee was not paid within the time limit specified in the invitation.

☐ No protest accompanied the payment of additional search fees.

Group A: claims 1-11

A magnetic resonance imaging (MRI) system comprising: a cavity adapted to interact with a spin ensemble in an imaging subject in a static magnetic field; a resonator adapted to generate an interaction between the cavity and the spin ensemble that increases polarization of the spin ensemble; and a control system operable to acquire a magnetic resonance signal from the imaging subject.

Group B: claims 12-19

A magnetic resonance imaging (MRI) method comprising: thermally insulating between an imaging subject and a cavity, the cavity being at a first temperature, the imaging subject being at a second, different temperature and containing a spin ensemble in a static magnetic field; generating an interaction between the cavity and the spin ensemble that increases polarization of the spin ensemble; and acquiring a magnetic resonance signal from the imaging subject.

The features common to both groups of claims include an MRI method and system comprising: a cavity, an imaging subject having a spin ensemble, and generating an interaction between the cavity and the spin ensemble to increase the spin ensemble polarization. Said features were already well known in the art at the claim date and therefore do not form a single inventive concept. The remaining features, namely a resonator (group A) and thermally insulating between the subject and the cavity (group B), are not linked by a single common inventive feature. Therefore, the claims lack unity of invention.

Patent Document Cited in Search Report	Publication Date	Patent Family Member(s)	Publication Date
US2001013779A1	16 August 2001 (16-08-2001)	None	
US6677751B1	13 January 2004 (13-01-2004)	DE19946371C1	13 June 2001 (13-06-2001)
		EP1089086A1	04 April 2001 (04-04-2001)
		EP1089086B1	28 December 2005 (28-12-2005)
		JP2001153938A	08 June 2001 (08-06-2001)
		JP3462846B2	05 November 2003 (05-11-2003)